

# Automatic docking of articulated vehicles

Student: Tony Hertogh  
0774745  
D&C report: 2017030

Supervisors: K. Kural MSc (HAN)  
dr.ir. I.J.M. Besselink (TU/e)

## Summary

Logistic centers currently rely on the skill of the truck drivers to drive their vehicle to the docking stations. For example, a limitation of a driver is the blind spot, where the driver cannot see behind the vehicle while driving in reverse. Automation of a tractor-semitrailer where the vehicle is driven in reverse autonomously can help with the limitations of truck drivers. To autonomously control the vehicle a controller and a reference path is need. Under assumption that the reference path is produced, an path following controller was defined. The controller generates a preview point generated behind the vehicle and reduces the distance between the preview point and the reference path. The path following controller is observed while acting on a reversing model of a tractor-semitrailer combination. The performance of following the reference path with minimum error is evaluated to assess the capability of the controller to control the vehicle. The tractor-semitrailer combination is modeled by use of a kinematic and dynamic model. The simulations have shown that the controller is capable of controlling the tractor-semitrailer combination in reverse within limits. For general 90 degrees corners with a radius above 10 meter the controller is fully capable to follow the reference path. Decreasing the radius results into an observable deviation to the reference path. When changing the vehicle combination from a tractor-semitrailer to a double semi-trailer combination, the controller was still capable of controlling the vehicle to the reference path with certain deviations.

## Table of Contents

Summary .....	2
1. Introduction.....	4
2. The Kinematic model .....	5
3. Controller.....	7
4. Kinematic translation .....	12
5. Simulation tests kinematic model.....	15
6. Multibody model.....	20
7. Limitations/disturbances.....	33
8. Double articulated vehicle combination .....	40
9. Conclusions & recommendations.....	46
10. References.....	48
Appendix A: Single Articulated Vehicle.....	49
Appendix B: Articulated model variables.....	52
Appendix C: Single articulated vehicle for reversing .....	53
Appendix D: Noise simulations on multibody model.....	56

# 1. Introduction

In the Intralog project automation of trucks for multiple scenarios is evaluated. In particular, automated inter-terminal transport and autonomous docking and coupling of trucks is aimed for. Autonomous docking a truck consists of two parts; optimal reference path generation for the truck to follow and a closed loop controller to make the truck follow the generated reference path. Assuming an optimal reference path is available, a path following controller is proposed to guide the truck to the docking station. The path following controller generates the steering angle for the truck based on the current position and orientation of the truck.

The goal of this report is to test the proposed controller for a variety of models to evaluate the performance of its capability to follow a given reference path. It is tested on multiple reference paths and optimum controller variables have been found.

The outline of the report consists of multiple sections, starting with the simulation model that is used to analyze the motion of the vehicle is discussed. It consists of three parts: a kinematic model of a single articulated vehicle, a driver model and a kinematic translation needed to control the vehicle. The kinematic model is tested with the controller to see if there are limitations and the performance of the controller with respect to path following is evaluated. A multibody model is introduced and the path controller is iteratively tuned to find the optimum response. Disturbances on input signals are tested to find the limitations of the controller. The controller is then tested on an expanded kinematic model having two articulation points to find the capabilities of the controller for a longer vehicle combination. Finally the results of multiple scenarios consisting different reference paths and different controller gains which have been tested are discussed and recommendations are given.

## 2. The Kinematic model

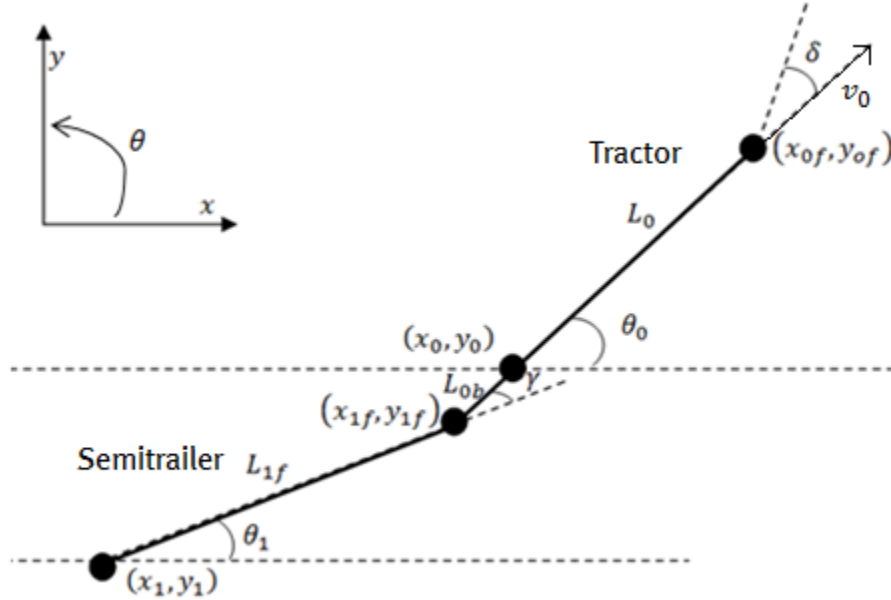


Figure 1: Single articulated vehicle model

A kinematic model is a model describing the motion of points without considering mass of the objects or the force working on the objects in the model. Based on geometrical relationships, the movement of the system can be described [1]. The vehicle in the setup consists of a tractor with one front axle and one rear axle, a trailer with one axle and a kingpin point, connecting the tractor with the trailer. Figure 1 shows the tractor-semitrailer setup.

The kinematic model is a single track model, assuming one fixed point at the axles of the tractor and trailer. The steering angle  $\delta$  at the front of the tractor is an input to the model. The longitudinal velocity  $v_0$  is the second input to the model, defined at the reference point  $(x_0, y_0)$ . The heading angle of the tractor and semi-trailer are indicated by  $\theta_0$  and  $\theta_1$  respectively. The articulation angle  $\gamma$  is equal to the difference in heading angle between tractor and semi-trailer.  $L_0$  is the wheelbase of the tractor,  $L_{ob}$  is the distance between rear of the tractor and the kingpin  $(x_{1f}, y_{1f})$  and  $L_{1f}$  is the distance between the kingpin and the axle of the semi-trailer  $(x_1, y_1)$ .  $L_{ob}$  will be negative for a normal tractor-semitrailer combination.

The kinematic model is based on the constraint that the wheels on the axles have no sideslip. The general form of the non-holonomic constraint is:

$$\dot{x} \sin(\theta) - \dot{y} \cos(\theta) = 0 \quad (2.1)$$

$\dot{x}$  and  $\dot{y}$  are the velocities of the axles in the given coordinate system and  $\theta$  is the angle with respect to the x-axis. Using Equation 2.1, the non-holonomic constraints for the model in Figure 1 are given by:

$$\dot{x}_{0f} \sin(\theta_0 + \delta) - \dot{y}_{0f} \cos(\theta_0 + \delta) = 0 \quad (2.2)$$

$$\dot{x}_0 \sin(\theta_0) - \dot{y}_0 \cos(\theta_0) = 0 \quad (2.3)$$

$$\dot{x}_1 \sin(\theta_1) - \dot{y}_1 \cos(\theta_1) = 0 \quad (2.4)$$

To obtain the kinematic model, the positions equations of the axle points are differentiated and substituted in Equation (2.2)-(2.4) to obtain the yaw rates ( $\dot{\theta}_0, \dot{\theta}_1$ ):

$$\dot{\theta}_0 = \frac{v_0}{L_0} \tan(\delta) \quad (2.5)$$

$$\dot{\theta}_1 = \frac{v_0}{L_{1f}} \left( \sin(\gamma) - \frac{L_{0b}}{L_0} \tan(\delta) \cos(\gamma) \right) \quad (2.6)$$

$v_1$  can be determined based on Figure 2. It consist of two components; a direct component of  $v_0$  and a second component from  $\theta_0$ .

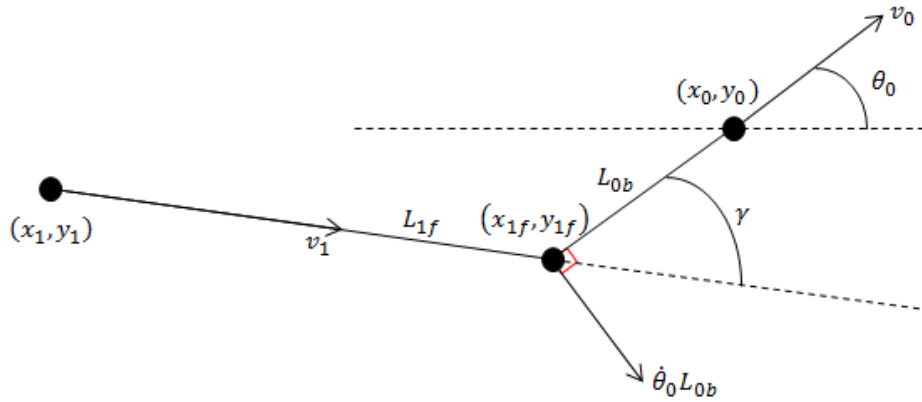


Figure 2: Longitudinal speed  $v_1$  components

From Figure 2, Equation 2.7 can be obtained.

$$v_1 = v_0 \cos(\gamma) + \dot{\theta}_0 L_{0b} \sin(\gamma) \quad (2.7)$$

With the inputs of system,  $v_0$ ,  $v_1$  and  $\delta$ , initial conditions for the heading angles of tractor and semi-trailer and the initial position of the vehicle, the equations of the kinematic model can be implemented in a simulation model. Detailed derivations of equations and parameters of the kinematic model are found in Appendix A and B respectively. The equations for the position, velocity, yaw and yaw-rate are solved to define the kinematic model in the simulation environment.

### 3. Controller

The controller is a path-following controller which aims to follow a reference path. The reference path is an input provided externally by a path planner and calculated beforehand. It consists of a series of two (x,y) coordinates which define a path. The concept of the controller as shown in Figure 3. The input for the controller consists of the kingpin position, axle position of the semi-trailer and the longitudinal speed of the semi-trailer. The output of the controller is the desired front wheel steer angle for the vehicle. The path following controller is mainly used for a reversing motion of the tractor-semitrailer combination.

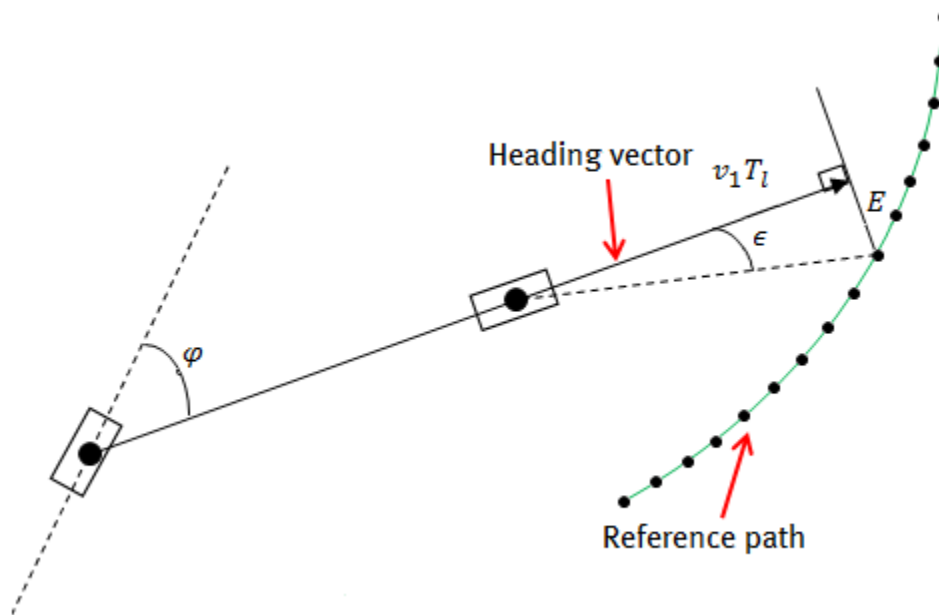


Figure 3: Controller principle

As input processing the position of the kingpin and the semi-trailer axle are converted into a 'heading' vector. The heading vector consists of two parts: direction and magnitude. As seen in Figure 4, the direction of the heading vector is equal to the trailer vector and this vector is normalized to be a unit vector. Equation 3.1 calculates the magnitude of the heading vector ( $L_v$ ) based on the longitudinal velocity ( $v_1$ ) which has a controllable input, the look ahead time ( $T_l$ ).

$$L_v = v_1 T_l \quad (3.1)$$

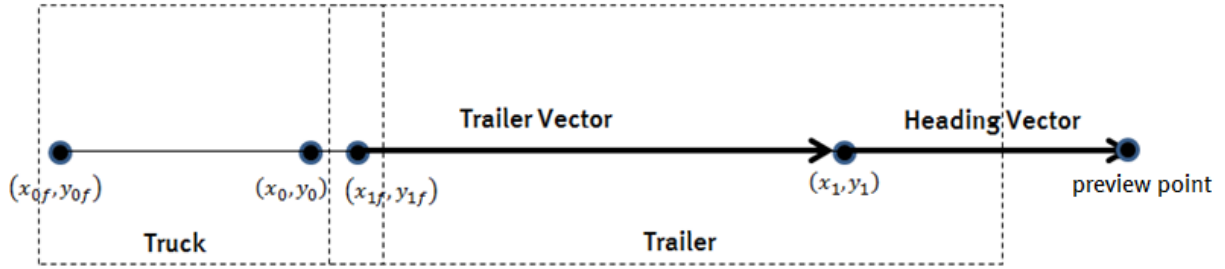


Figure 4: Schematic view of defining the heading vector

With the heading vector, a preview point is defined from which controller operates. For every point in the reference path (Rf), the distance between the preview point and the reference path points is calculated to find the minimum distance. For every time step, the closest reference point is found. To reduce computation, a variable ‘*l*’ is introduced to represent a range of reference points, depending on the previous optimal point. A schematic view of this principle is shown in Figure 5.

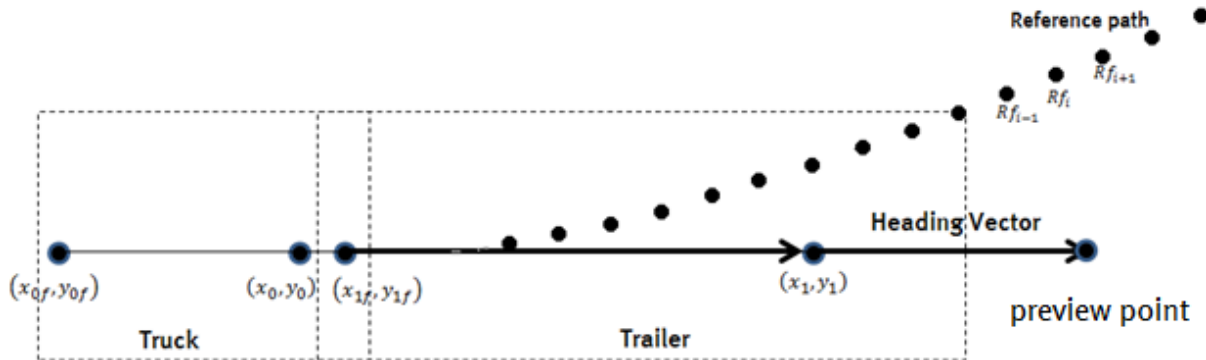


Figure 5: Schematic view of the path following calculation

Vector calculus can be used to find the orthogonal distance from any preview point to the reference point. In this case, the reference path points are fixed points with a relative distance between each other. A problem occurs when the closest reference point is not orthogonal to the preview point, as seen in Figure 6. To solve this problem, two vectors  $a_1$  and  $a_2$  are created to find the orthogonal distance.



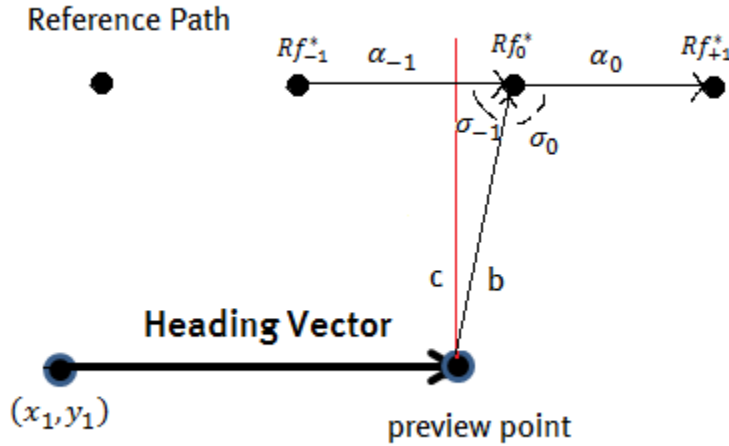


Figure 6: Reference point problem

Vector  $b$  in Figure 6 is the vector with the distance from the preview point to the optimal reference point  $Rf_0^*$ . The points  $Rf_{-1}^*$  and  $Rf_{+1}^*$  are the points near the optimal point. With vector  $c$  and the heading vector desired angular rotation can be calculated. The vectors  $a_1$  and  $a_2$  can be calculated with Equation 3.2.

$$a_i = Rf_i^* - Rf_{i-1}^* \quad \text{for } i = 0,1 \quad (3.2)$$

To find the orthogonal vector, the vector  $b$  is projected on vector  $a_1$  and  $a_2$  :

$$\cos(\sigma_i) = \frac{a_i \cdot b}{a_i \cdot a_i} \quad (3.3)$$

$\sigma_i$  is the angle between the vector  $a_i$  and  $b$ . If  $\sigma_i$  is within 0 and 90 degrees, an orthogonal vector  $c$  can be found by:

$$|c| = \|b - \alpha_i a_i\| \quad (3.4)$$

To calculate the angle in radians between the heading vector and the orthogonal vector, the following trigonometric identity is used:

$$\varepsilon = \text{sign}(c) \cdot \arctan\left(\frac{|c|}{L_v}\right) \quad (3.5)$$

To reduce the distance between the preview point and the reference path, the angle  $\varepsilon$  must be reduced. To obtain a steering input for the vehicle,  $\varepsilon$  is multiplied with a second controller gain, the steering sensitivity ( $K_s$ ). The output of the path controller is given by Equation 3.6.

$$\varphi = K_s \varepsilon \quad (3.6)$$

For reversing motion, this output is defined as the desired angle to move the rear semi-trailer axle to the reference point. The semi-trailer has no steerable axle. Therefore a kinematic translation from  $\varphi$  to the steering input of the tractor  $\delta$  must be defined. For forwards motion  $\varphi$  is equal to  $\delta$ .

The path controller has two parameters. The *'lookahead'* preview time influences the magnitude of the heading vector. With increasing value for the look ahead time, the magnitude of the heading vector is increased and the path controller uses reference path points further away from the semi-trailer rear axle. Deviations of a straight path reference, for example a curve, are observed earlier. The controller can anticipate the change in curvature, and provide a smoother response. The upper limit for the value of the look ahead preview time is reached when deviations of a straight path are ignored by the controller or the reference is slowly followed, which can be seen in the right figure of Figure 7. The path controller will be very sensitive at the lower limit so the controller is not able to properly create a heading vector. It will not be able to create a realistic input for the kinematic model, which can turn it into an instable vehicle as shown in the left figure of Figure 6.

The steer sensitivity is the second parameter to influence the controller. This parameter directly influences the output of the controller. Increasing the value for the steer sensitivity results into a more direct response on the desired input of the kinematic model. An example of the upper limit is shown in Figure 8. The controller overcompensates the steering angle and the movement of the tractor moves into an oscillation motion. At the lower limit, the tractor barely responds to the output of the controller due to a low steering sensitivity.

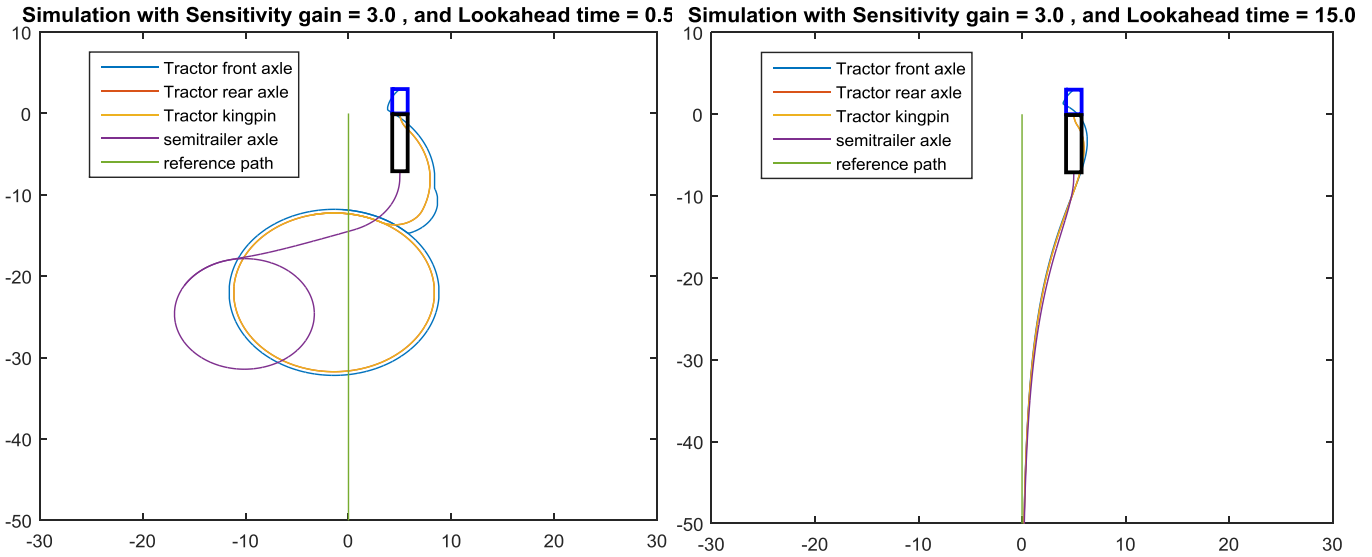


Figure 7: Upper (left) and lower (right) limit on the look ahead time

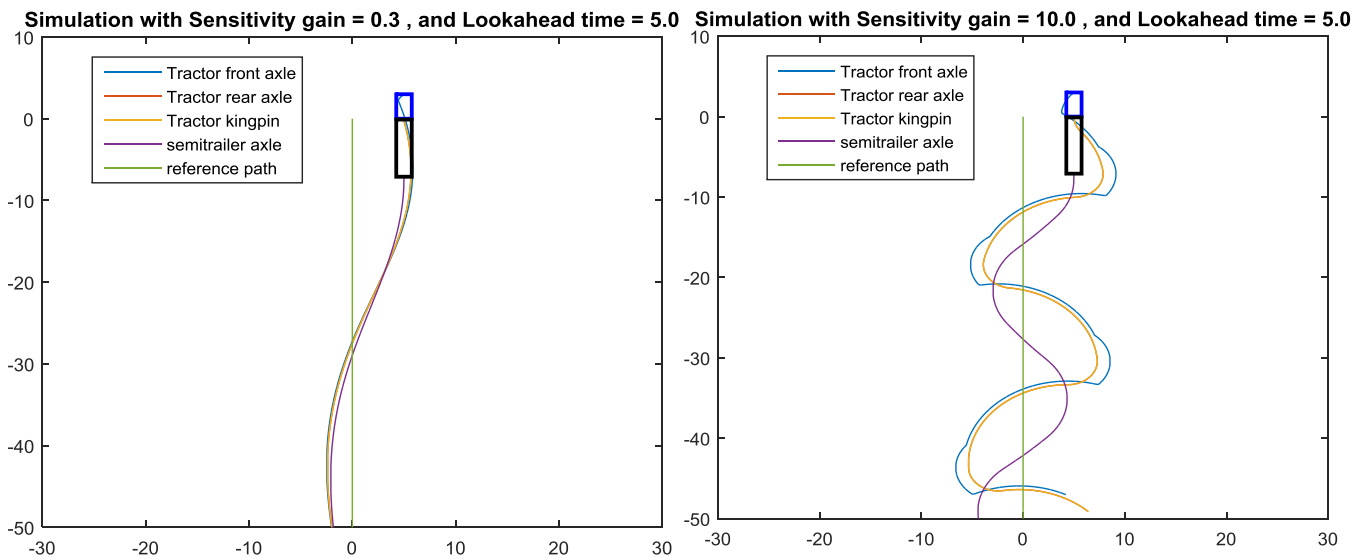


Figure 8: Upper (right) and lower (left) limit on the steering sensitivity

Initially there were no limitations for the actuator in the steering wheel implemented. An actuator has a limited operating speed. To simulate the limited operating speed, the derivative of the output of the controller is taken and it is saturated to 1 rad/s (Full steering motion in one second). The saturated derivative is integrated to obtain the output of the controller.

## 4. Kinematic translation

The kinematic model has one steering input  $\delta$ . However the path controller gives the desired angle  $\varphi$  and the rear axle when reversing the tractor-semitrailer combination is not a steered axle. Therefore, through a kinematic relation, the desired  $\delta$  can be determined to minimize the positional error between the semi-trailer axle and the reference path.

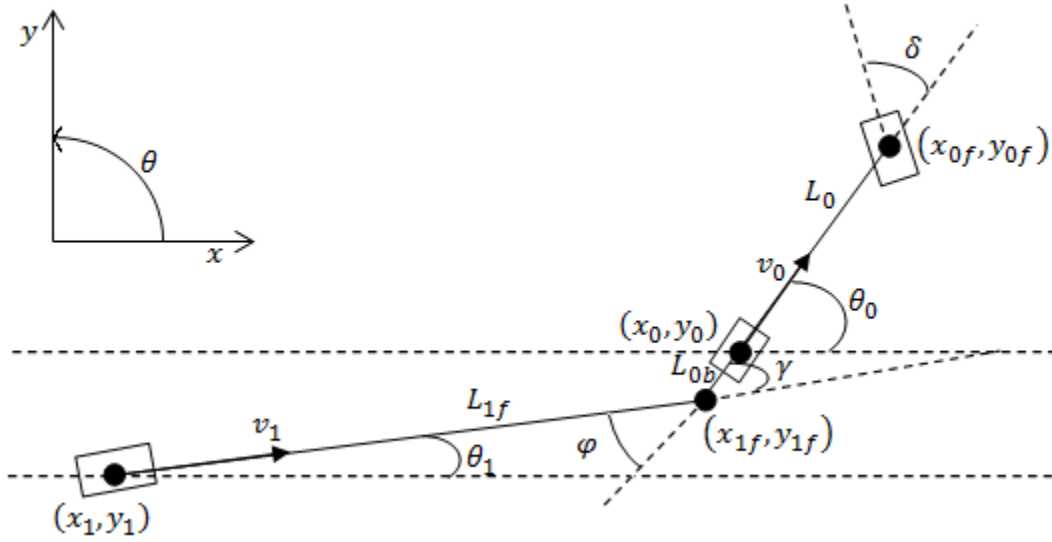


Figure 9: Tractor-semitrailer model

Using a kinematic model of a single articulated vehicle for reversing, the reference point is  $(x_1, y_1)$  instead of  $(x_0, y_0)$  for the standard single articulated vehicle model.

While driving in reverse, Equations 4.1 and 4.2 can be derived as shown in Appendix C.

$$\dot{\theta}_1 = \tan(-\varphi) \left( \frac{-v_1}{L_{1f}} \right) \quad (4.1)$$

$$\dot{\theta}_0 = \frac{v_1 \sin(\gamma) - \dot{\theta}_1 L_{1f} \cos(\gamma)}{L_{0b}} \quad (4.2)$$

For reverse motion of the tractor-semitrailer combination, a non-linear translation from the output of the controller  $\varphi$  to the steering input of the tractor  $\delta$  is needed. Given the original kinematic model of Chapter 2, Equation 2.5 can be written as:

$$\delta = \arctan \left( \frac{L_0 \dot{\theta}_0}{v_0} \right) \quad (4.3)$$

Substituting Equation 4.2 into 4.3 results into:

$$\delta = \arctan \left( \frac{L_0 \frac{v_1 \sin(\gamma) - \dot{\theta}_1 L_{1f} \cos(\gamma)}{L_{0b}}}{v_0} \right) \quad (4.4)$$

Equation 4.1 can be substituted into Equation 4.4:

$$\delta = \arctan \left( \frac{L_0 \frac{v_1 \sin(\gamma) - \tan(-\varphi) \left( \frac{-v_1}{L_1 f} \right) L_1 f \cos(\gamma)}{L_0 b}}{v_0} \right) \quad (4.5)$$

Equation 4.5 can be simplified to:

$$\delta = \arctan \left( \left( \frac{L_0 v_1}{L_0 b v_0} \right) (\sin(\gamma) + \tan(-\varphi) \cos(\gamma)) \right) \quad (4.6)$$

Equation 4.6 shows the relationship between the output of the controller  $\varphi$  and the steering input of the tractor  $\delta$ . To verify Equation 4.6, a linearized case where  $\gamma$  and  $\varphi$  are small is considered.

Equation 4.7 is valid for small  $\gamma$  and small  $\varphi$ , shown in Figure 10.

$$\delta^* = \gamma - \varphi \quad (4.7)$$

Assuming there is no side-slip on the vehicle axles, Equation 4.8 can be defined.

$$\delta^* = \frac{L_0 b}{L_0} * \delta \quad (4.8)$$

Combining Equation 4.7 and 4.8 results into Equation 4.9.

$$\delta = \frac{L_0}{L_0 b} (\gamma - \varphi) \quad (4.9)$$

To validate that Equation 4.6 and 4.9 are equal, Equation 4.6 can be linearized for small  $\gamma$  and  $\varphi$  and it shows that Equation 4.6 and 4.9 are equal. A second validation has been done by evaluating the controller with the kinematic model using diverse reference paths.

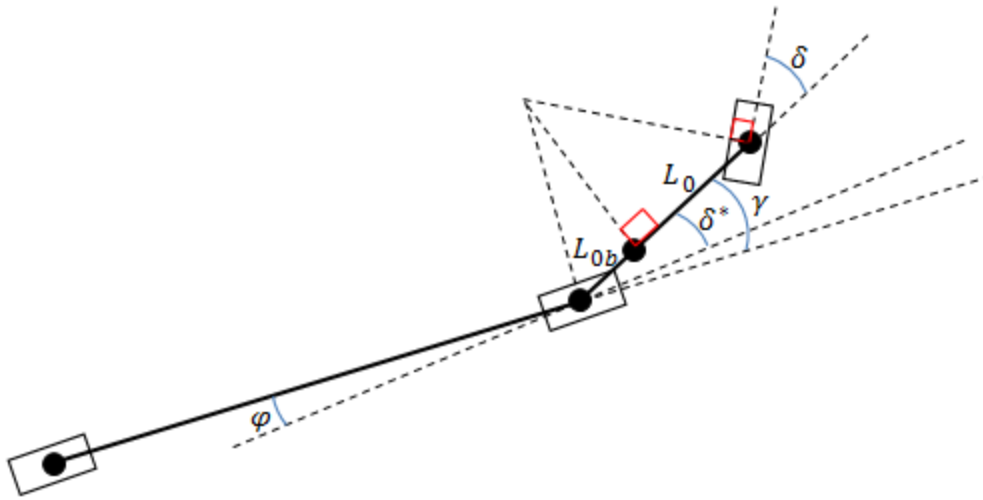


Figure 10: Linearized tractor-semitrailer model

## 5. Simulation tests kinematic model

To test the controller capabilities, several scenarios are tested to validate the controller and models performance. All the simulations in this Chapter are done with  $v_0 = -1m/s$  (reversing motion) and the dimensions are given by:  $L_0 = 3.8, L_{1f} = 7, L_{0b} = -0.2$ . The kinematic model is subjected to several tests to make sure the controller is working and there are no issues with the kinematic model. If the controller works on a kinematic model, the controller can be tested on more advanced models. To find a limitation on the reference path, a 180 degree turn is generated. The reference path is created by a forward driving model turning 180 degrees with a maximum steering angle of 42 degrees. This scenario is used to analyze the performance of the controller and its capability to perform difficult maneuvers. The simulation result for the tractor in reverse along given reference path is shown in Figure 11. Note that the controller gains are not fully optimized at this point. However, a problem is seen at the end of the simulation. Figure 12 shows the angular positions of the vehicle. The articulation angle converges to zero which means the axel positions should be on a vertical line. The heading angle of the tractor converges to 180 degrees which corresponds with the vertical reference line. However, as seen Figure 13, the axle positions do not verify this data.

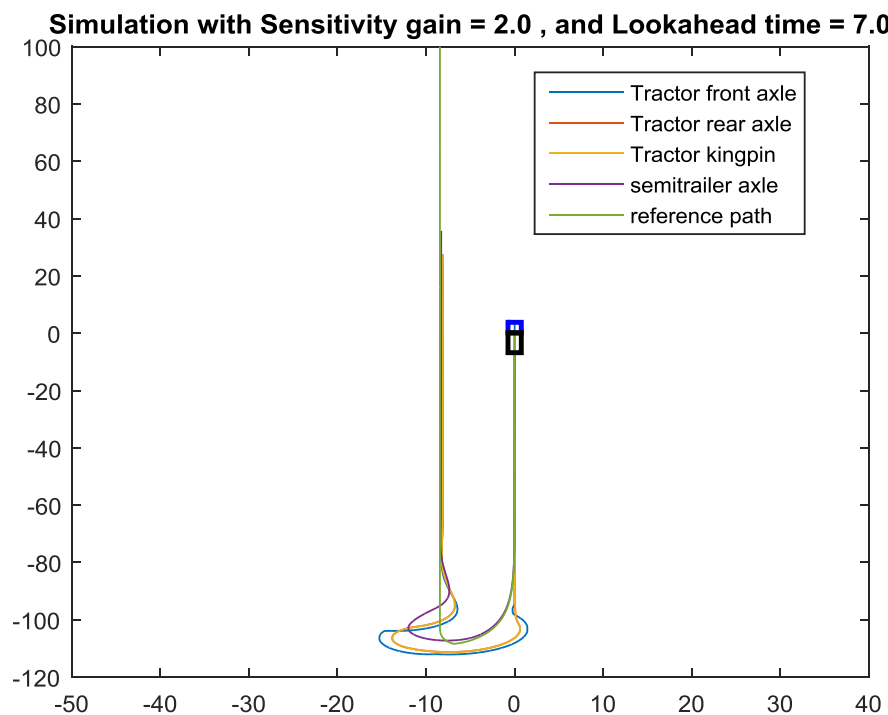


Figure 11: Simulation result with extended straight path

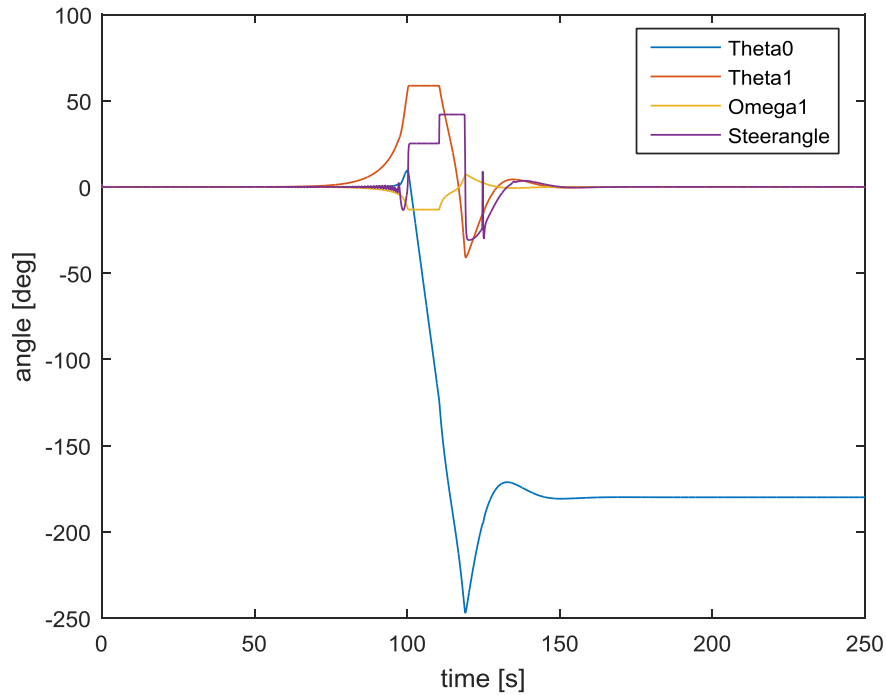


Figure 12: Heading, steering and articulation angle of the vehicle during simulation

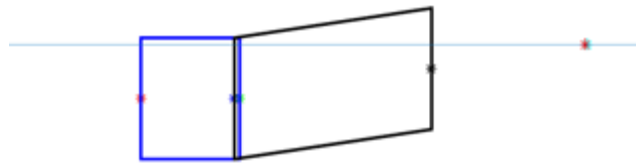


Figure 13: Tractor-trailer position at t=250 [s]

The reason for this error is found at the calculation of the positions of the trailer, which is based on integrating the velocities of the trailer. The position of the axle of the trailer is calculated by:

$$x_1 = \int -v_1 \sin(\theta_1) dt \quad (5.1)$$

$$y_1 = \int v_1 \cos(\theta_1) dt \quad (5.2)$$

Obtaining the position by integrating the velocity when the time step is not infinite small can result into a position deviation per time step. If the velocity changes in the time step, an error on the position is found. When the position is directly calculated through the position of the tractor and the articulation angle, the deviation disappears. The position of trailer axel of the kinematic model is given by:

$$x_1 = x_0 - L_{0b} \cos(\theta_0) - L_{1f} \cos(\theta_1) \quad (5.3)$$

$$y_1 = y_0 - L_{0b} \sin(\theta_0) - L_{1f} \sin(\theta_1) \quad (5.4)$$



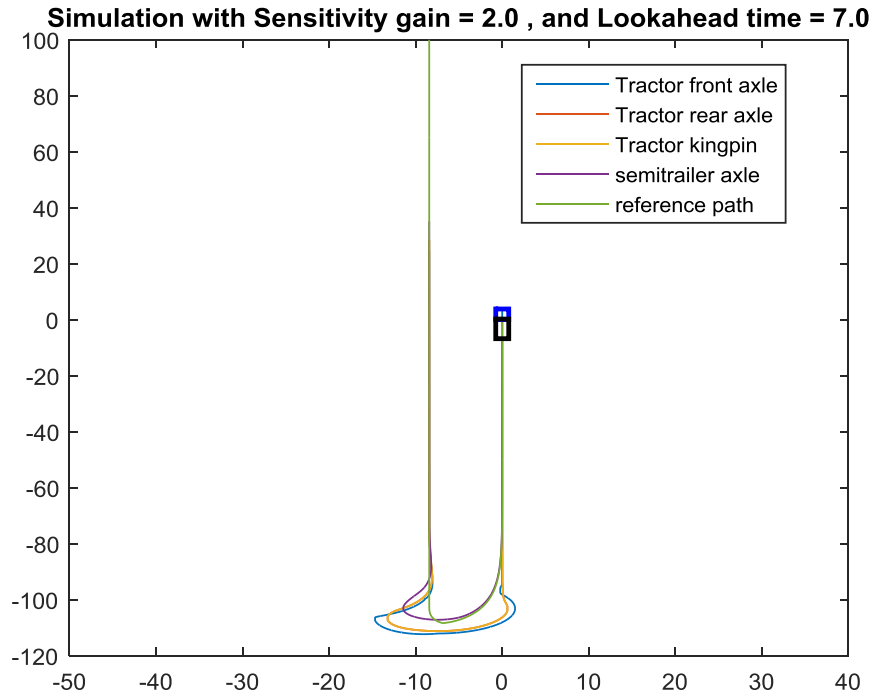


**Figure 14: Simulation using improved trailer model <sup>{Kinematic model}</sup>**

The result is shown in Figure 14. As can be seen, the position lines up with the rest of the vehicle, meaning the lateral deviation on the position is solved. It also shows that the controller cannot cope with 180 degrees without overshooting the reference path. A limitation is found on the controller. The turn is changed to a 90 degrees turn; this is a maneuver that the tractor must be able to perform since it is a common maneuver while docking a tractor-semitrailer combination. A new forward simulation reference path was made using a 90 degrees turn. The maximum steering angle was 50 degrees. The reference path and the result of the simulation are shown in Figure 15. To test the performance of the controller, the reference path is followed in reverse. As seen the vehicle is capable to follow the trajectory, even with limited steering angle. The deviation in distance between the rear axle of the tractor and the reference path in the curvature is at maximum 1 meter. It shows that the controller is fully capable to perform a standard maneuver. However the deviation to the reference path is large (as shown in Figure 14).

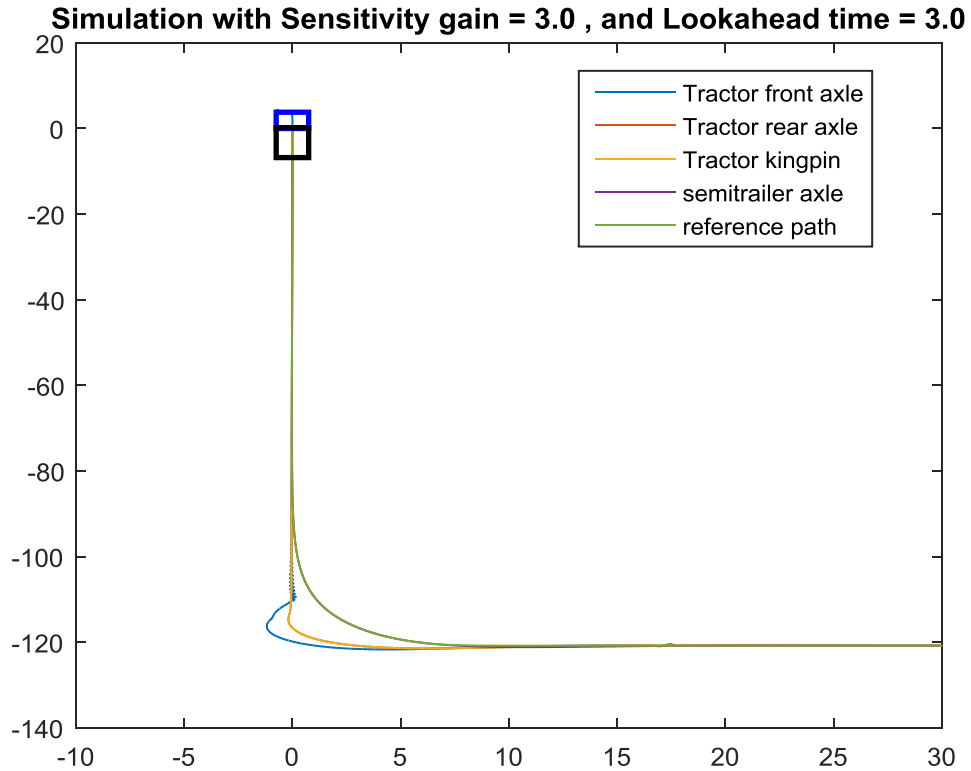


**Figure 15: Simulation result of vehicle reversing the path starting at the endpoint**

To find a limit for the controller, a reference path was made using a maximum steering of 60 degrees. The reference path and the simulation result of the reverse movement are shown in Figure 16. The control parameters are adjusted to give decent response and there is no limit on the steering angle in this simulation.

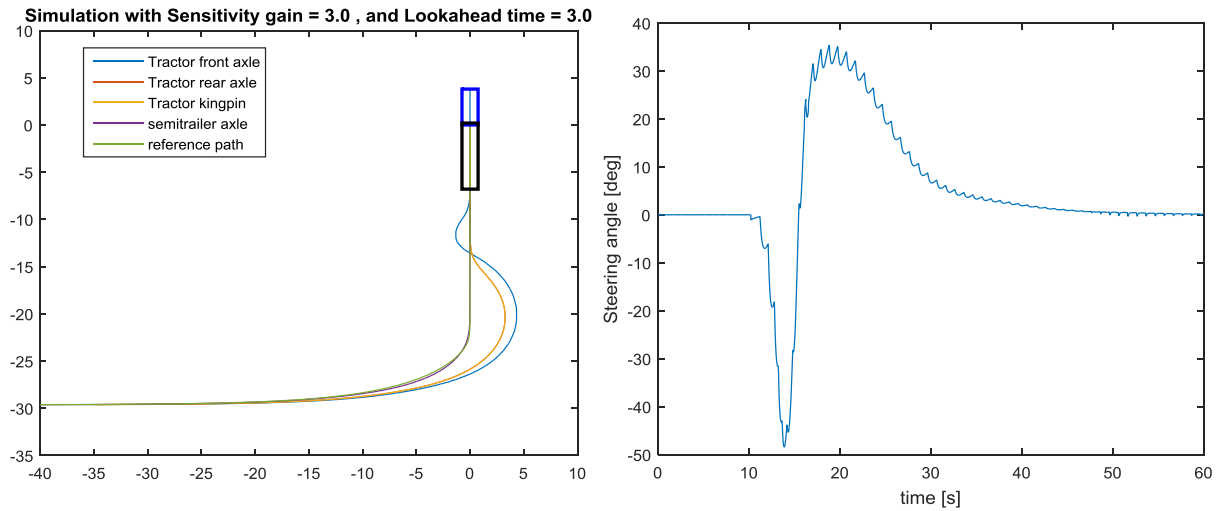


Figure 16: Reverse simulation with 90 degree corner <sup>{Kinematic model}</sup>

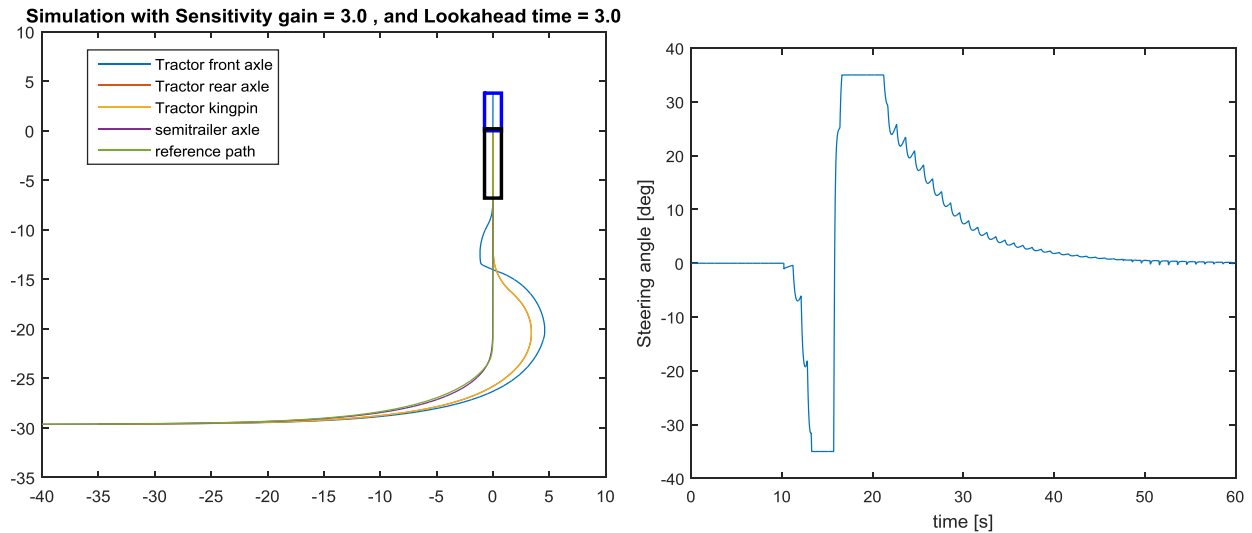


Figure 17: Reverse simulation with 35 degree limit

Figure 17 shows the same simulation but now with limit on the steering angle. The oscillations in Figure 16 and Figure 17 are caused by non-optimized control gains. The limit of the steering angle to control the vehicle in a 90 degree corner is 35 degrees. The steering angle can be reduced to nearly half the value needed for the vehicle to perform the maneuver in forwards motion. It shows that the controller is fully capable to control the rear axle to a reference path, even under restriction of the steering angle.

## 6. Multibody model

The kinematic model shows promising results with regards to the controller performance. However, since the kinematic model is purely vector based modeling with a no-slip condition, the controller has to be tested on a multibody model. The multibody model is included with a non-linear tyre model and a much more accurate representation of a real tractor-semitrailer combination; it is presented and given as a working model. A 3D image of the tractor-semitrailer is shown in Figure 18.

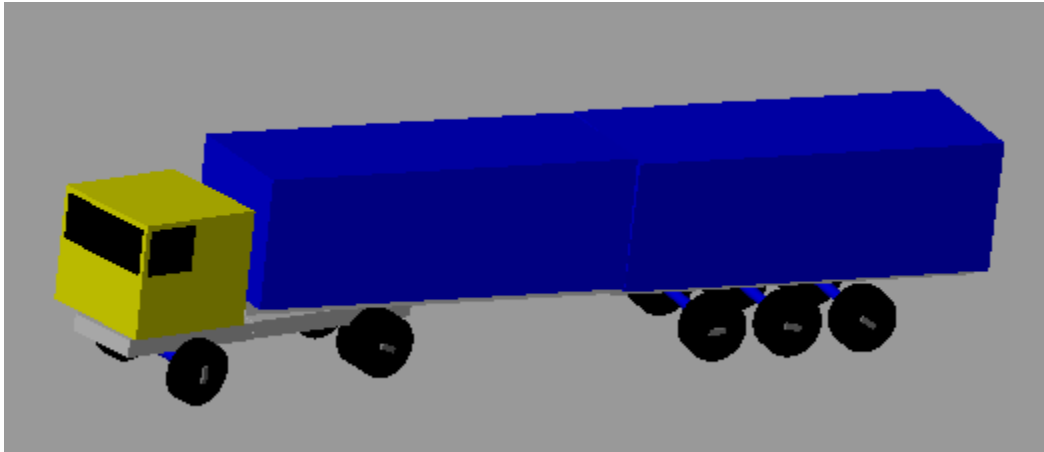


Figure 18: 3D Image of multibody model

To show the difference between the kinematic model and the multibody model of the tractor-semitrailer a steer input of 0.25 rad is given to both models simultaneously and the result is plotted in Figure 19 and Figure 20. As seen both models have similar responses with an identical input. Due to the more detailed modeling of the components of the articulated vehicle in the multibody model, its response is different. As seen in Figure 20, as result of the non-linear behavior of the multibody model, oscillations can occur which will have effect on the controller. To have two models that have identical dimensions, the parameters of the kinematic model are adjusted to match the multibody model. The wheelbase of the tractor ( $L_0$ ) is changed to 3.8 meter, The distance between the rear tractor axle, the kingpin ( $L_{0b}$ ) is changed to -0.74 meter (the axle is placed in front of the rear axle of the tractor) and the wheel base of the trailer ( $L_{1f}$ ) is changed to 8.475 meter. The change in parameters will be definitive for the rest of the report to generate proper comparisons with the multibody model.

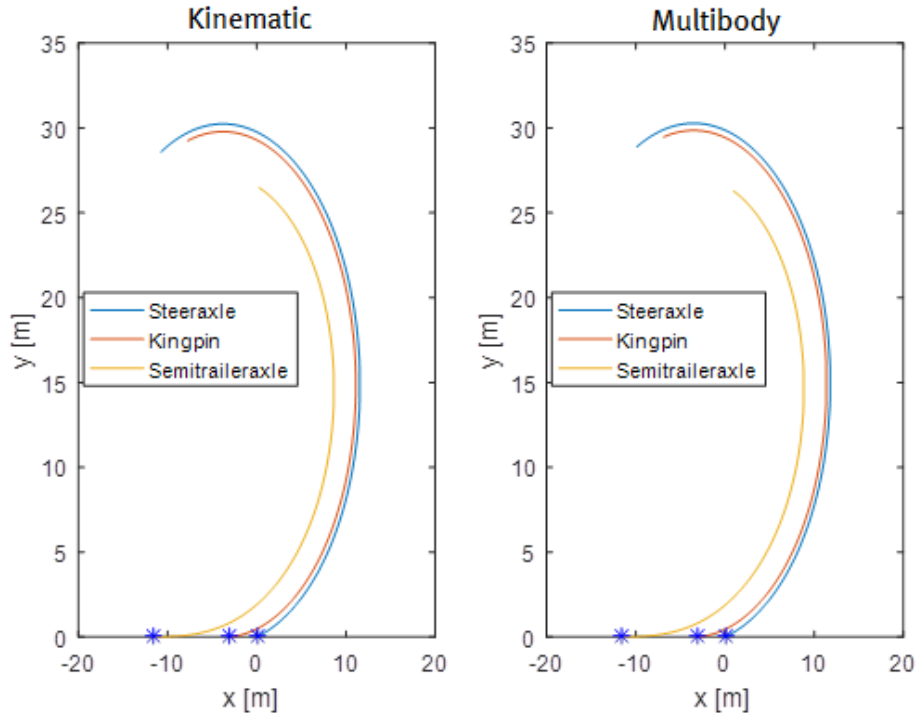


Figure 19: Positions of Kinematic and multibody model with a fixed input

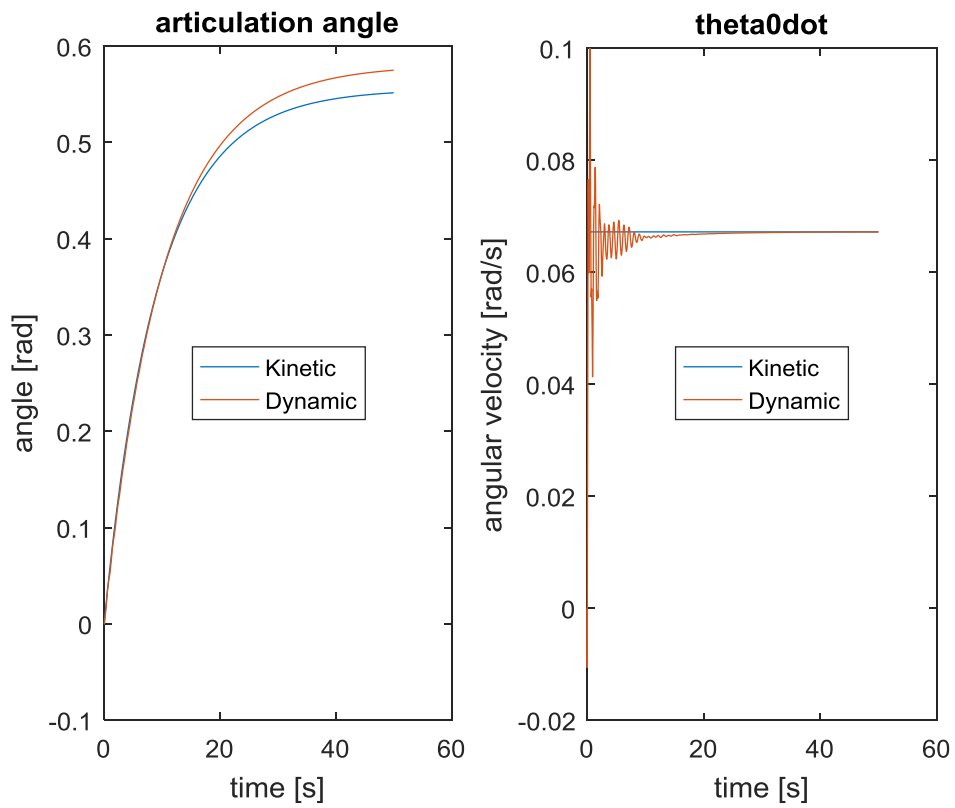


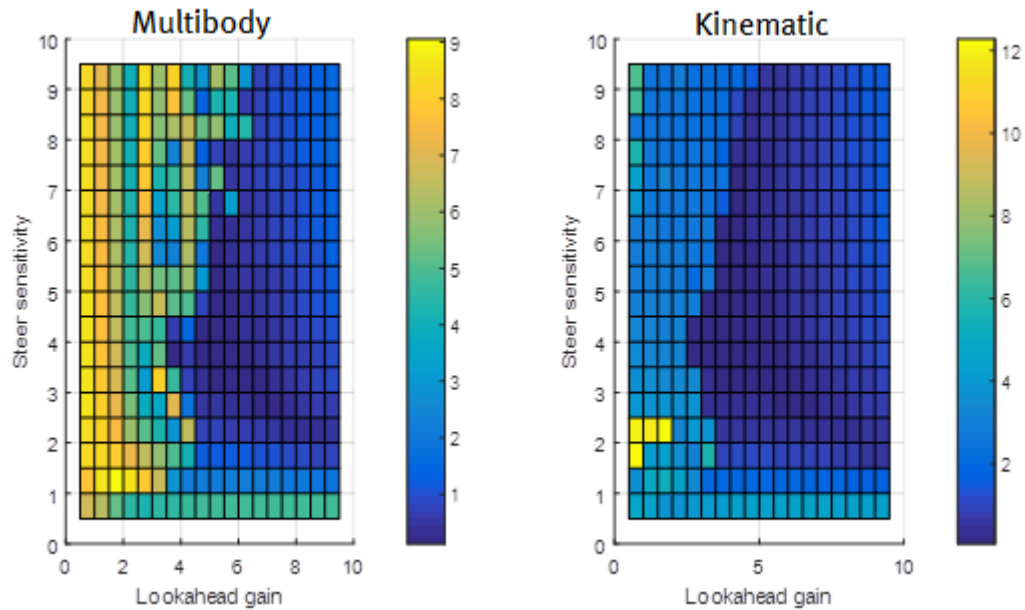
Figure 20: Angle and angular velocity of Kinematic and multibody model with a fixed input

The multibody model was slightly adjusted to obtain the inputs for the controller. The input for the controller consists of the articulation angle of the vehicle, the yaw velocity of the tractor, the positions of the axles of the trailer and the reference path. The output of the controller is the steering angle which is applied to the multibody model. The reference path with which the multibody model is tested consists of 45 and 90 degrees corners. These corners are the general maneuvers for docking of a tractor-semitrailer combination, so it is important that the controller is capable to follow the given reference path. The results of three different reference paths are shown and are discussed at the end of the chapter.

The first reference path is a 45 degrees corner with a radius of 10 meter and the vehicle is following it in a reverse motion with a speed of 1 m/s. The results are shown in Figure 21 and Figure 22. Every point in the plot is the result of one simulation Figure 21 is a plot of the maximum error encountered at every simulation. Figure 22 shows the response at the optimum gains which are shown in Table 1. The plotted value is the maximum distance during the simulation between the rear axle of the trailer and the reference path. It is defined as stated in Equation 6.1.

$$E_m = |\max(Rf^* - R_a)| \tag{6.1}$$

$E_m$  is the error as discussed before,  $Rf^*$  is the vector of all closest reference points at each time step during the full simulation and  $R_a$  is the vector of coordinates of the rear axle of the trailer at



each time step.

Figure 21: Looped simulations for a 45 degrees corner with radius 10

	Steer sensitivity	Look ahead gain	$E_m$ [m]
Optimum Multibody	3.5	5.5	0.1252
Optimum Kinematic	3.5	4.5	0.0643

Table 1: Optimum controller gains for a 45 degrees turn with a radius of 10 meter

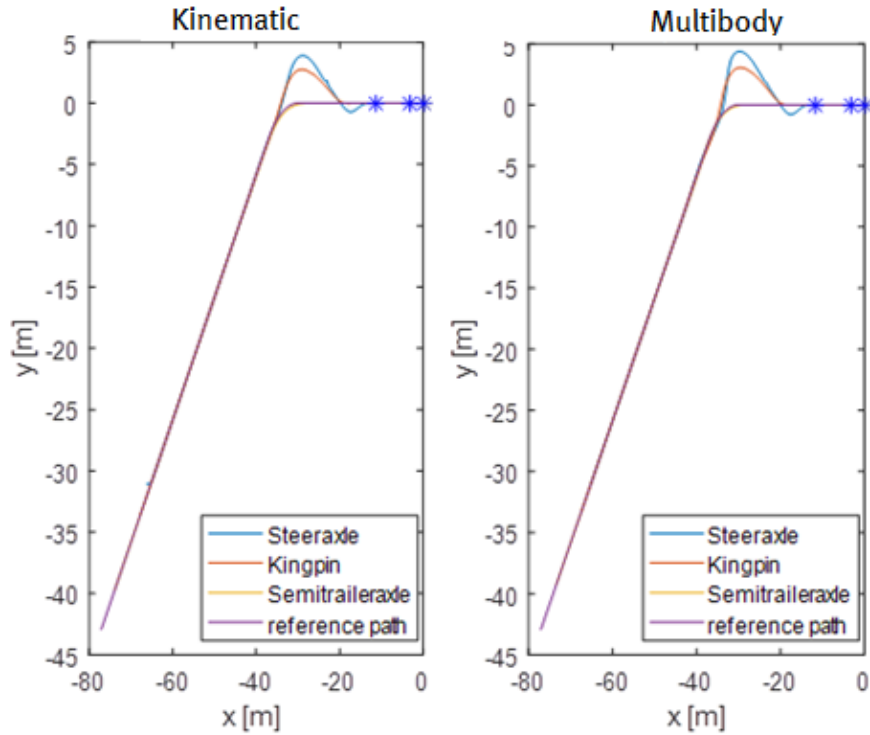


Figure 22: Simulation result for 45 degrees corner with optimum values (Kinematic and Multibody combined)

The second reference path is a 90 degree turn with a radius of 10 meter. The result is shown in Figure 23 and Figure 24. Similar to the previous test, the maximum distance during the simulation between the rear axle of the trailer and the reference path and the response at optimum gains is plotted. Table 2 shows the optimum gains that minimize the error for the second reference path.

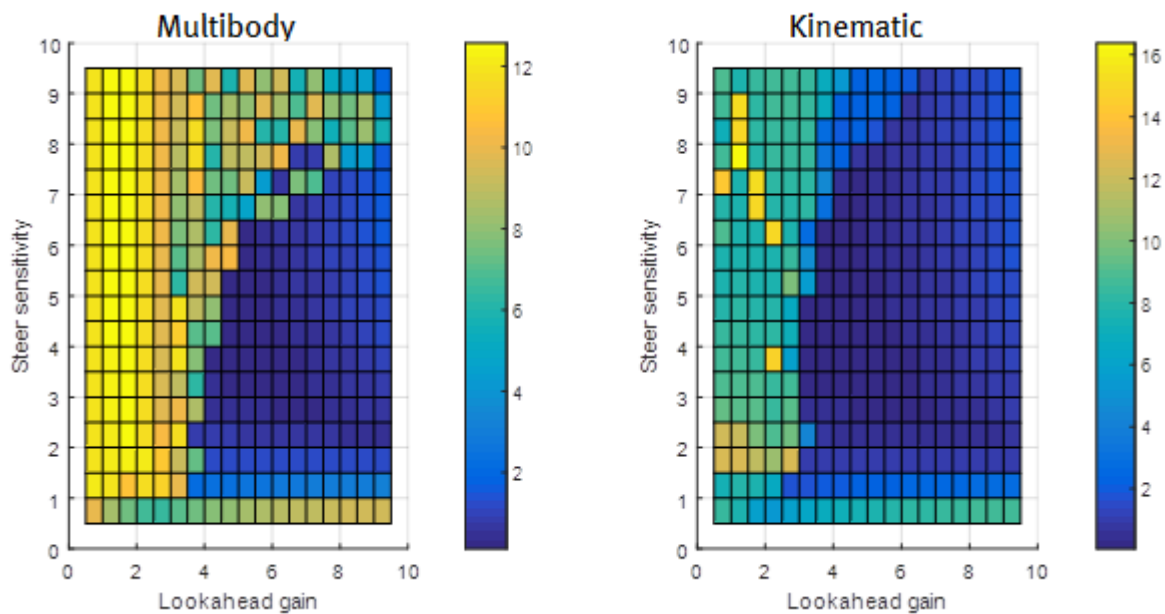


Figure 23: Looped simulations for a 90 degree corner with radius 10

	Steer sensitivity	Look ahead gain	$E_m$ [m]
Optimum Multibody	3.5	5.0	0.1186
Optimum Kinematic	3.5	4.5	0.0633

Table 2: Optimum controller gains for a 90 degrees turn with a radius of 10 meter

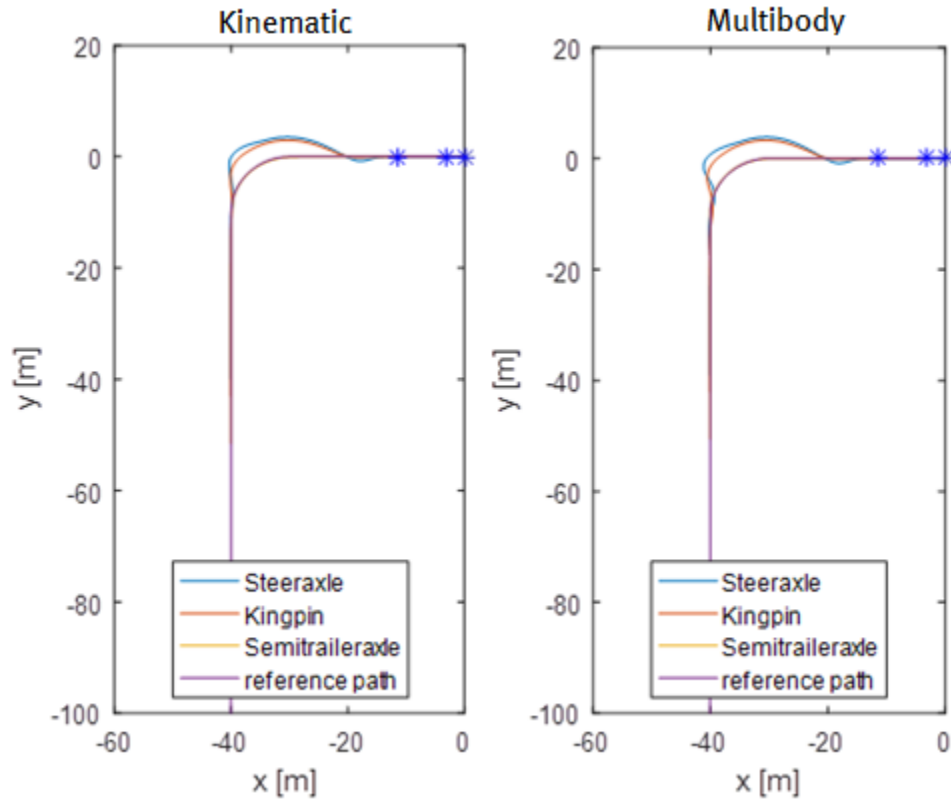


Figure 24: Simulation result for a 90 degree corner with radius 10 with optimum values <sup>{Kinematic and Multibody combined}</sup>

The third reference path is a 90 degrees turner with a radius of 15 meter. The result is shown in Figure 25 and Figure 26. Similar to the previous tests, the maximum distance during the simulation between the semi-trailer axle and the reference path and the response at optimum gains is plotted. Table 3 shows the optimum gains that resulted for the third reference path.



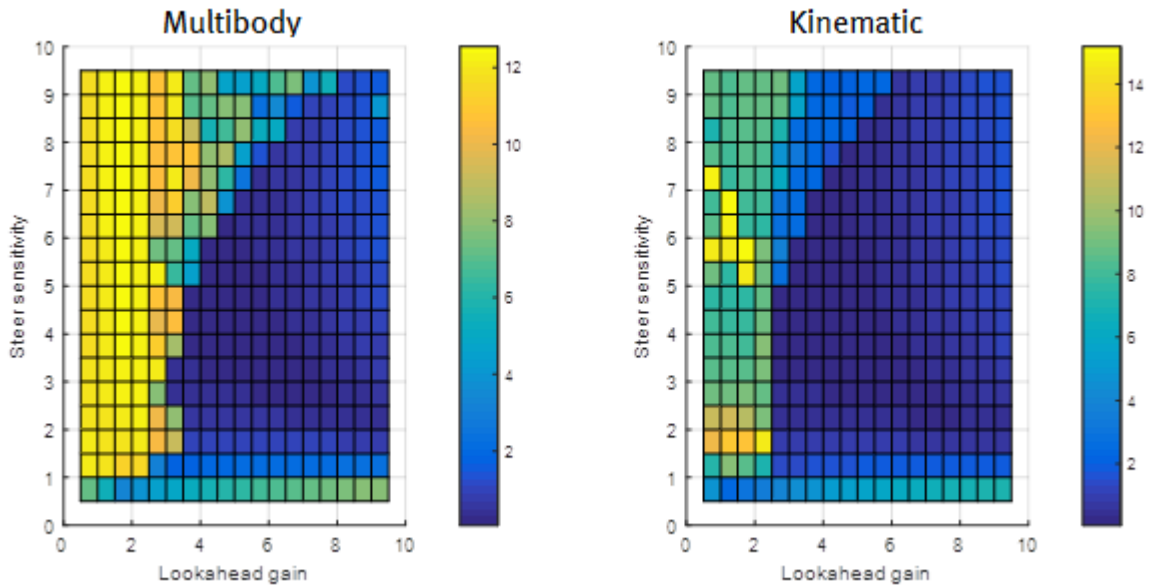


Figure 25: Looped simulations for a 90 degree corner with radius 15

	Steer sensitivity	Look ahead gain	Max error [m]
Optimum Multibody	3.5	5.0	0.0614
Optimum Kinematic	3.5	4.0	0.0504

Table 3: Optimum controller gains for a 90 degrees turn with a radius of 15 meter

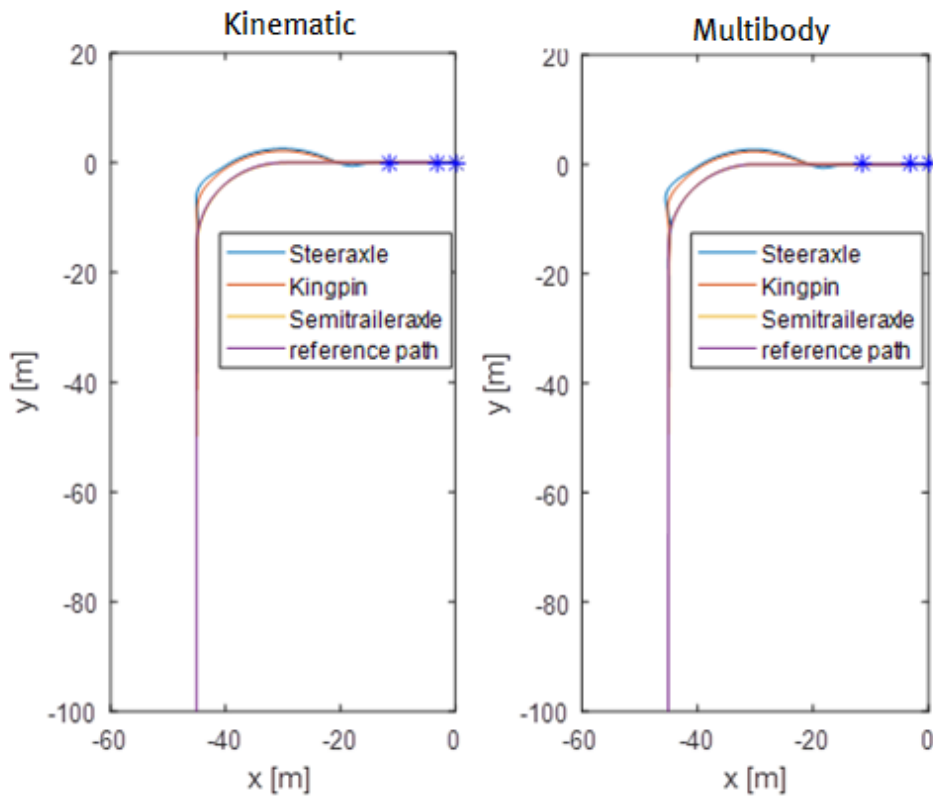


Figure 26: Simulation result for a 90 degree corner with radius 15 with optimum values

To recap the simulations, for all three reference paths there are gains that lead to an unstable vehicle (yellow areas in the looped simulation plots), in any case there is always a set of stable controller gains. The optimum values for the kinematic model and the multibody model are close to equal. The results of these simulations are not the final optimum values due to the fact that the vehicle must be able to follow a variety of reference paths. The three reference paths that are tested are simple maneuvers that the controller must be able to follow. It gives a general impression on stable and unstable controller gains and may reduce the amount of simulations to find optimum values.

A challenging reference path was defined and is shown in Figure 27. It consists of multiple corners with varying radius and degrees.

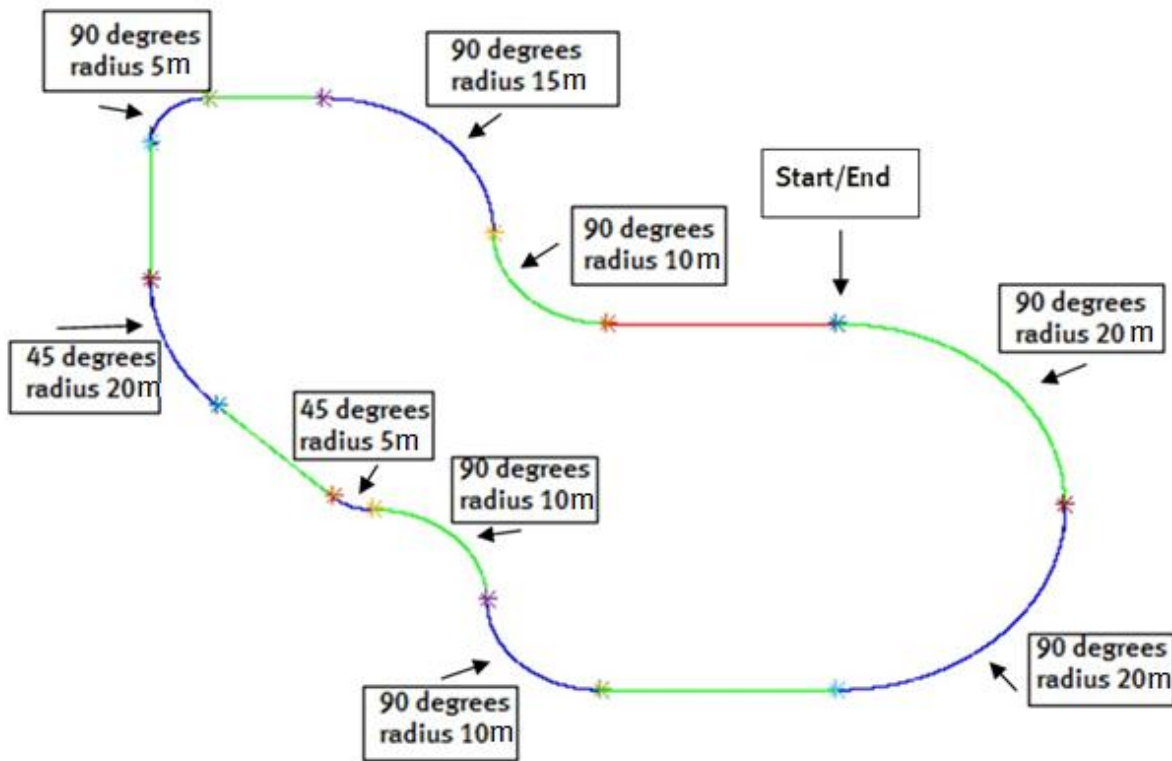


Figure 27: Challenging path for reverse vehicle

Multiple simulations are used in the same way as the single corners. To find the optimum controller gains, the simulation loops for the steering sensitivity between 1.5 and 6 and the look ahead time between 4 and 8.5. These are known to be stable for the single corner simulations. The error for the challenging path is determined by Equation 6.2:

$$E = \sum((|c| * v_1 * T)^2) \quad (6.2)$$

With  $|c|$  the absolute distance between the reference path and the semi-trailer axle,  $V_1$  the longitudinal velocity of the semi-trailer and  $T$  the sampling time of the simulation. The error represents the surface area of  $|c|$  shown in Figure 28. The error is plotted against the controller gains and is shown in Figure 29.

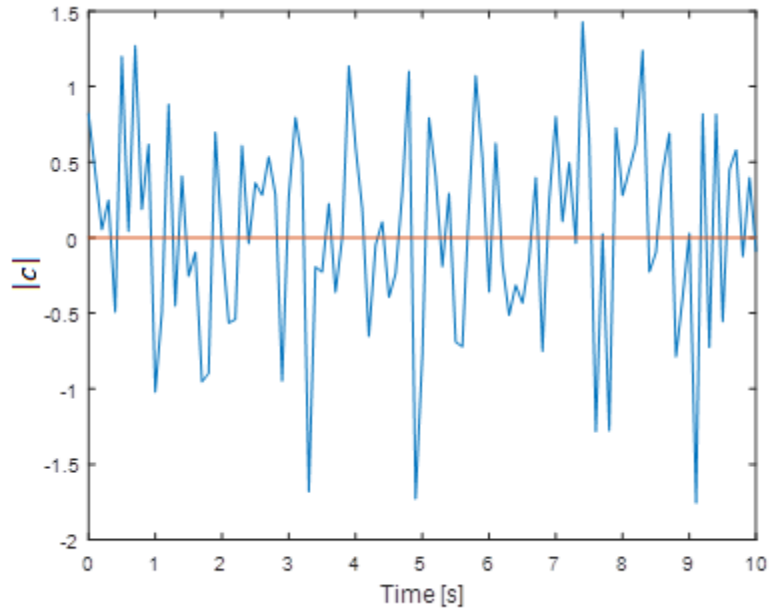


Figure 28: Error over time

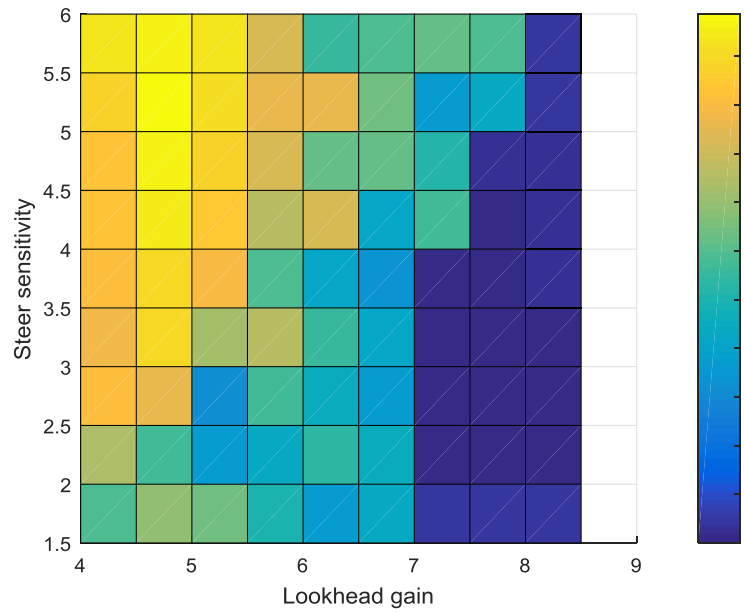


Figure 29: Result of looped simulations for reversing vehicle on the challenging path

The optimal controller gains with an accuracy of 0.5m are a steering sensitivity gain of 2.5 and a look ahead gain of 7.5. The table below shows the values near this point. Looking at values for the gains near the optimum point, the error decreases towards (2.5, 7.5). A local minimum is found.

Steering Sensitivity	Look ahead Gain	7	7.5	8
2		$21 \cdot 10^{-3}$	$16 \cdot 10^{-3}$	$12 \cdot 10^{-3}$
2.5		$5.2 \cdot 10^{-3}$	$4.9 \cdot 10^{-3}$	$7.6 \cdot 10^{-3}$
3		$7.1 \cdot 10^{-3}$	$11 \cdot 10^{-3}$	$19 \cdot 10^{-3}$

To increase the accuracy of the local minimum, a loop of simulations is done ranging the steering sensitivity from 2-3 and the look ahead gain from 7-8. The result is seen in the figure below. The best performance is found for a steering sensitivity of 2.6 and a look ahead gain of 7.3.

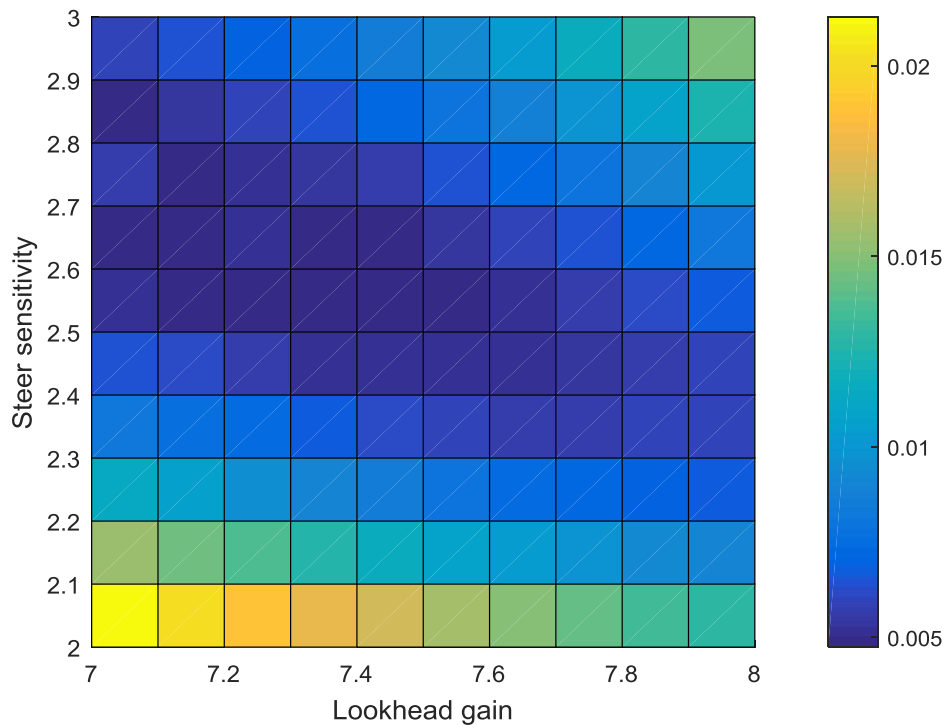


Figure 30: Looped simulation result for more accurate controller gains

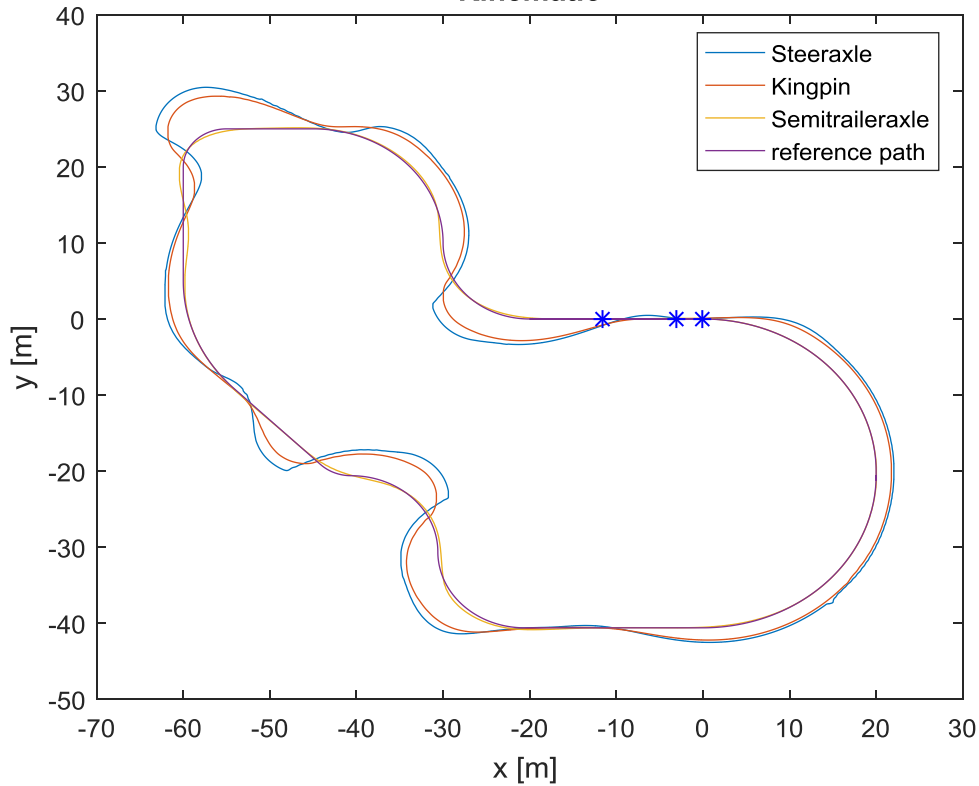


Figure 31: Simulation result of reversing vehicle with the optimal control gains <sup>{Multibody model}</sup>

The controller will be used for a docking maneuver with a tractor-semitrailer. These maneuvers consist of both forward and reverse driving. The optimum gain for driving in reverse is found, but the same controller cannot be used for driving forwards. Therefore, the same approach was used for forward driving.

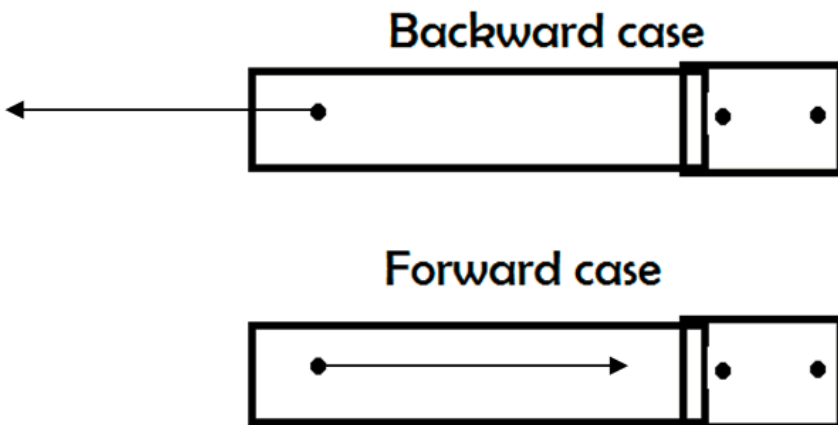


Figure 32: Controller setups

The general controller lay-out remains unchanged aside from the kinematic translation from the output of the controller to the steering input of the tractor. The translation is now given by Equation 6.3.

$$\delta = \varphi \quad (6.3)$$

The translation severely limits the response of the tractor-semitrailer since it cannot predict the reference path without a large look ahead gain. Considering the fact that the trailer follows the tractor when driving forwards, the controller will be limited to control the rear axle of the trailer to the reference path. Therefore a new but less challenging reference path was defined and is shown in Figure 33. It consists of several corners with different radiuses. The smallest radius is 12 m, which is found at the end of the path. The result of the looped simulations is found in Figure 34. The error is defined by Equation 6.2. The optimum is found at a steering sensitivity of 8 and a look ahead gain of 4 with an accuracy of 0.5. Surprisingly the optimum for the steering sensitivity was actually not near 8 when simulating with higher controller gains. A more accurate optimum is found for a steering sensitivity of 8.6 and a look ahead gain of 3.8 with an accuracy of 0.1. Figure 35 shows the error plotted against the control gains for the simulation. Figure 36 shows the simulation result using the optimal gains for forward driving. Two problems are shown in trajectory result. The first problem is the steady state deviation of approximate 0.5 m in the corners. Even with the optimal gains this problem cannot be removed. The steady state error is caused by the fact that the controller does not directly control the axel position but the preview point discussed at Chapter 3. Due to the limited capabilities of controlling the vehicle forwards with the semi-trailer axel position, this error will always be present. The tractor-semitrailer combination is easier to control when using the rear axle of the tractor but this can cause new problems in the reference path generation for the path planner. The second problem is the high steering sensitivity which can cause oscillating behavior as seen at the end of the simulation result in Figure 36. A small error leads to large inputs for the steering system.

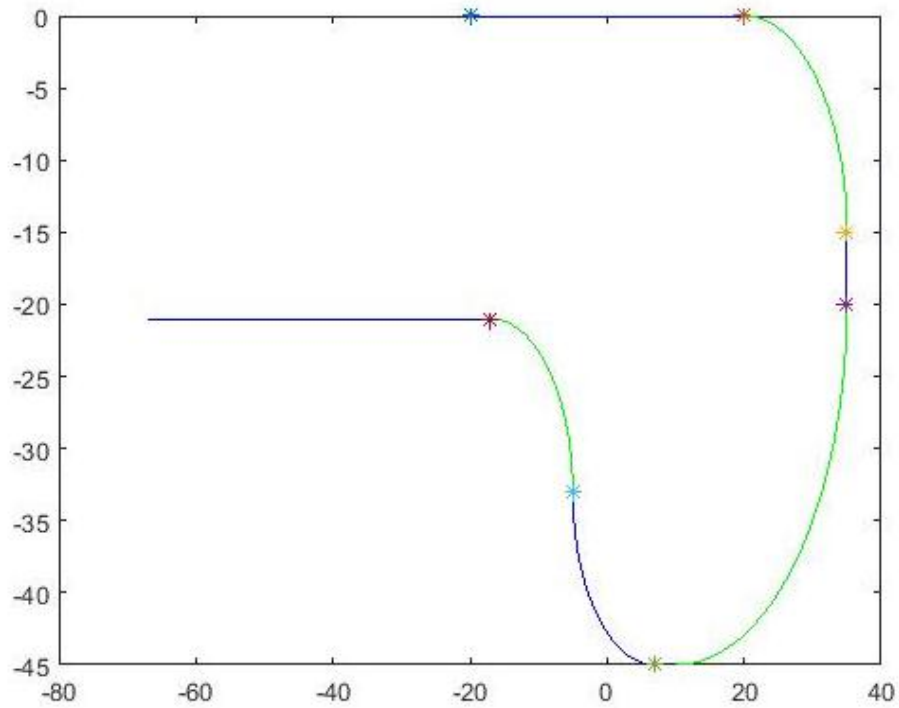


Figure 33: Forwards driving reference path

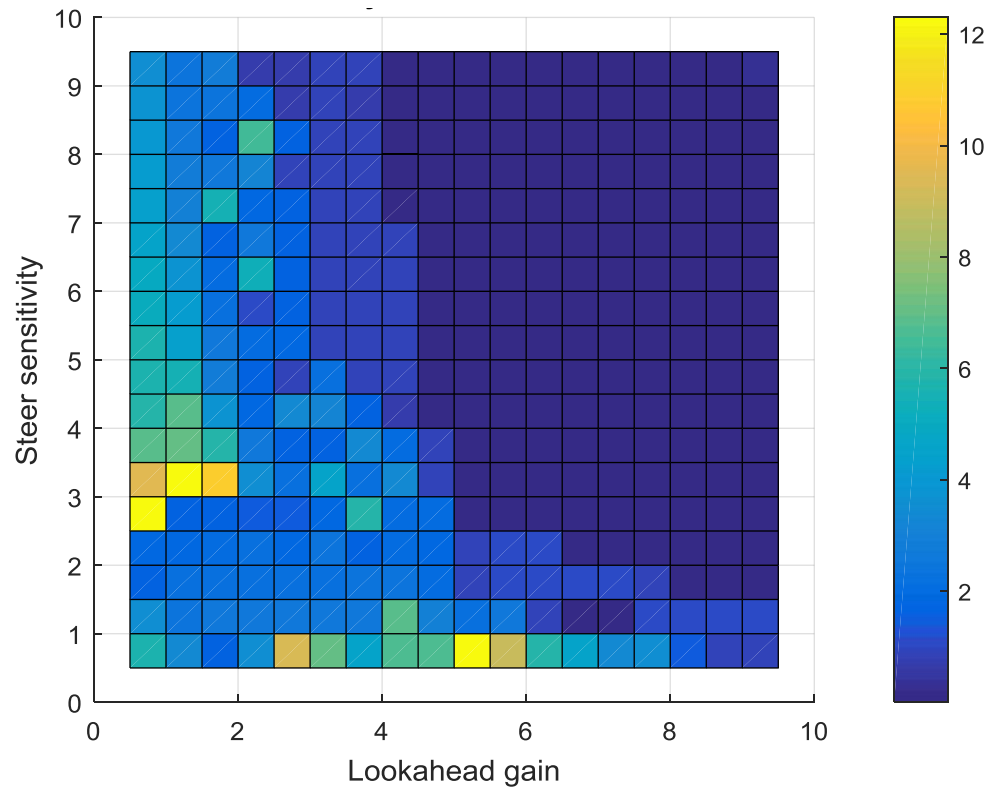


Figure 34: Result of looping simulations for forwards driving

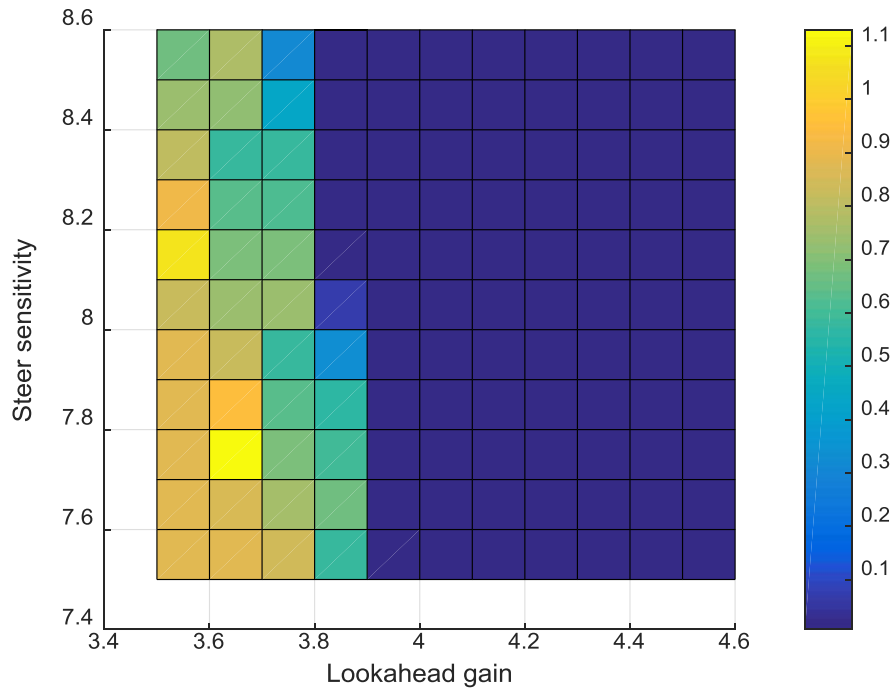


Figure 35: Accurate looping simulation result for forwards driving

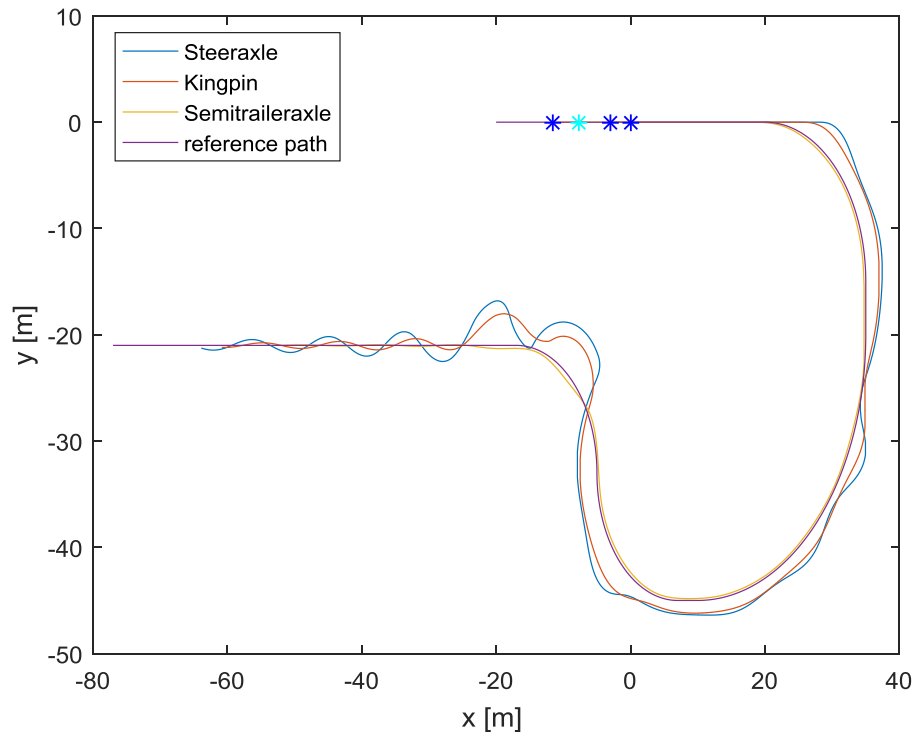


Figure 36: Simulation result of forwards driving with the optimal gains <sup>{Multibody model}</sup>



## 7. Limitations/disturbances

For the reversing tractor-semitrailer combination, certain limits of the controller are now being tested. All the following tests are done with the optimal controller gains for reversing; a steering sensitivity of 2.3 and a look ahead gain of 7.6. Figure 37 shows the limit of a lateral offset to the reference path. For proper behavior of the vehicle, the limit for the lateral offset is found near 1.8 m. The same test was done for radial offset; the orientation of the tractor-semitrailer has an offset around the z-axis. The result is shown in Figure 39. The limit was found to be 5.5 degrees, before the vehicle was unable to properly return to the reference path. When the offset is increased, the error is directly increased. Increasing error causes the steering angle to increase to its maximum steering angle. Eventually, when the maximum steering angle is needed for a certain time period to compensate for the error, the vehicle jack knifes.

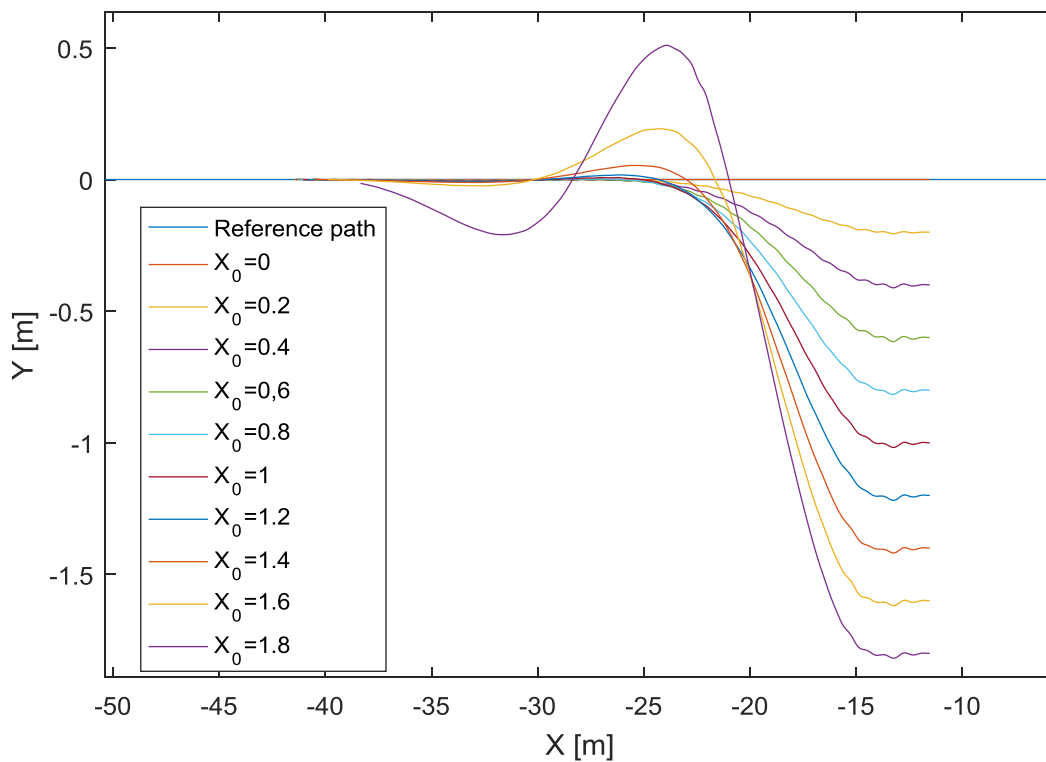


Figure 37: Y0 offset to reference path

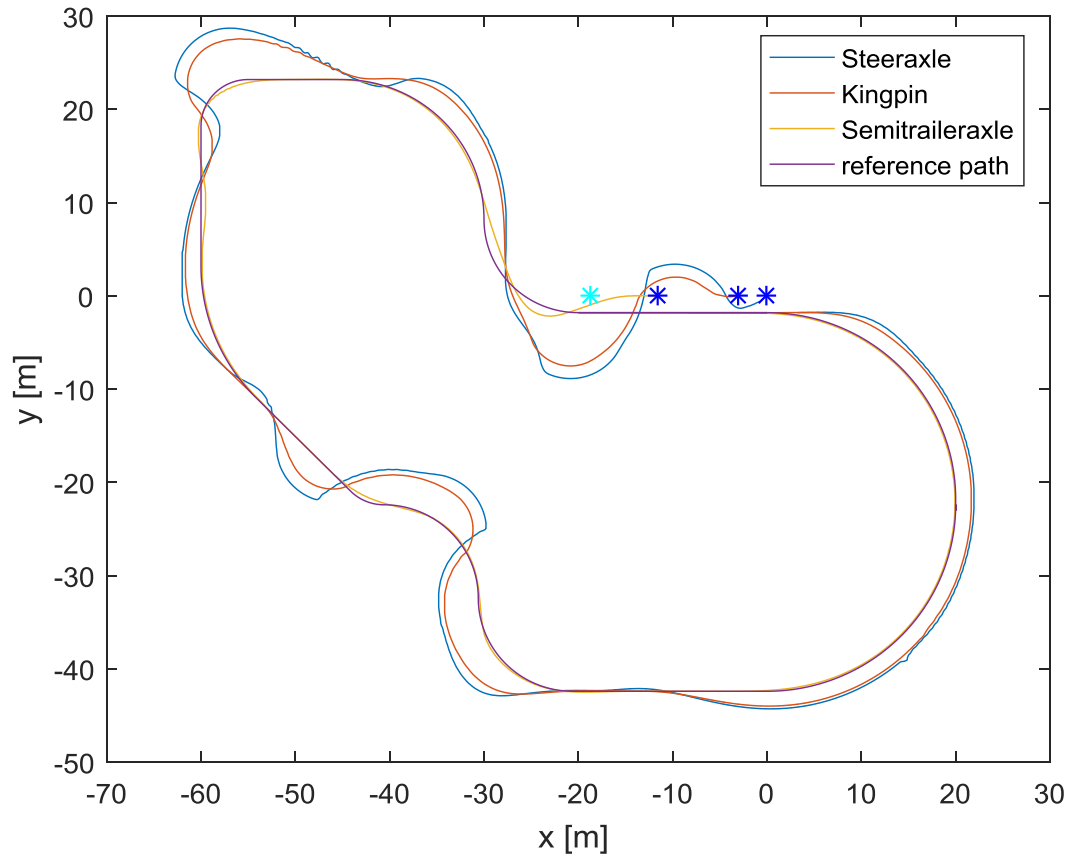


Figure 38: Simulation result with horizontal offset of 1.8m {Multibody model}

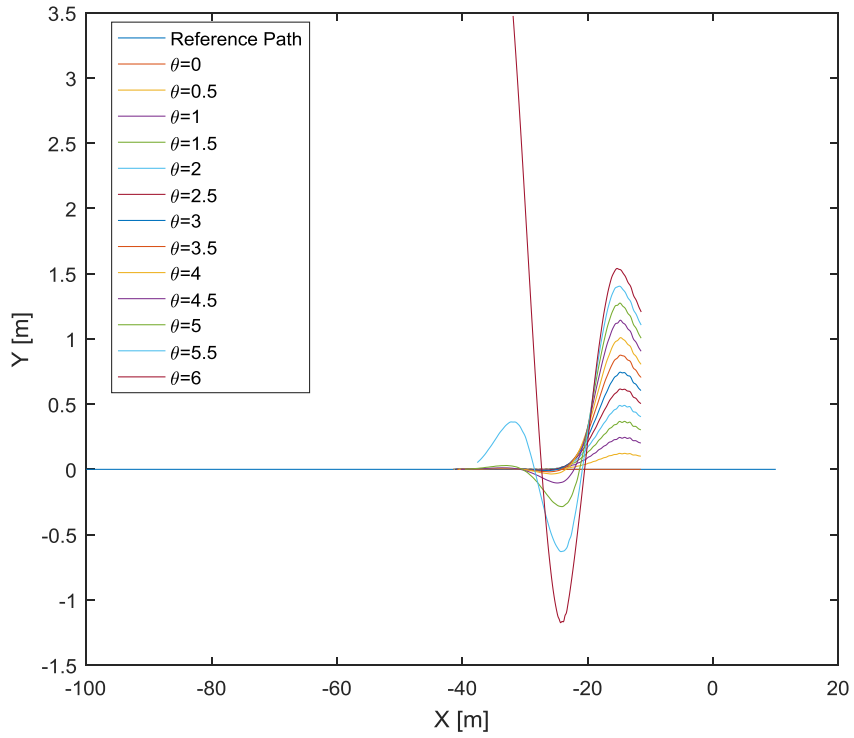


Figure 39: Angular offset to reference path

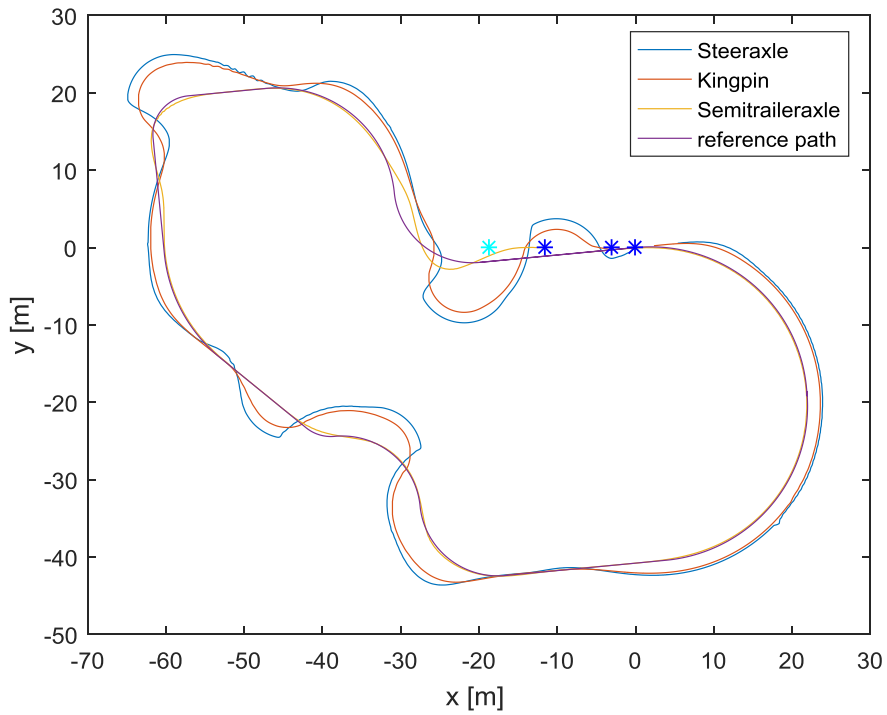


Figure 40: Simulation result with radial offset of 5.5 degrees <sup>{Multibody model}</sup>

Figure 41 shows simulation results of a combined lateral offset and the radial offset within the stable limits found before. Observed can be that for situations when the radial offset points to the reference path, the horizontal offset can be increased to stay stable and the opposite result can be found when the radial offset points away from the reference path. Overall it can be observed that a combined offset in both radial and horizontal direction has to be very limited in order to maintain stability. The system itself performs well when it comes to following the reference path. However when the initial offset becomes too large, the vehicle will become unstable.

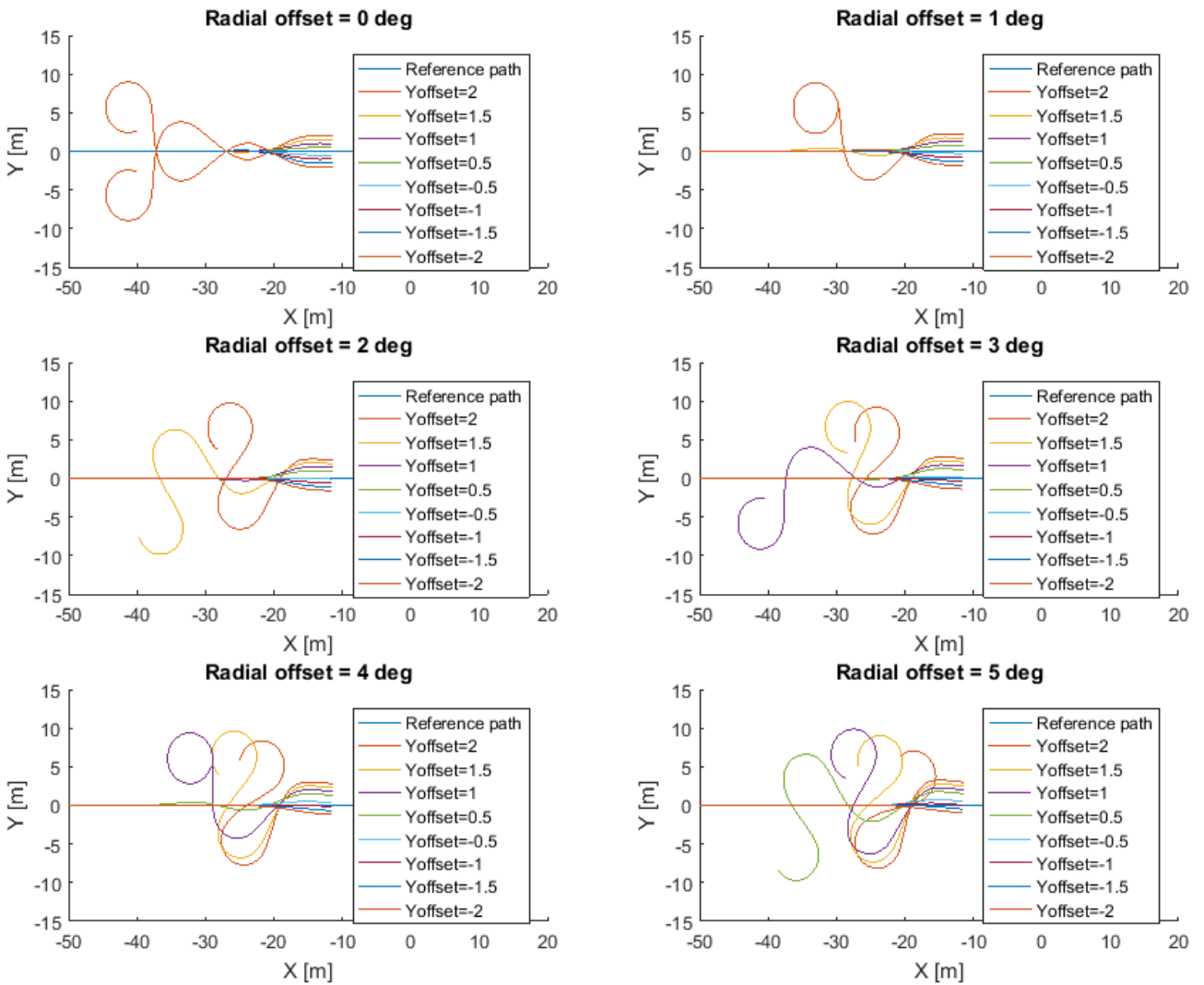


Figure 41: Combined offsets

The controller needs several inputs to calculate the steering angle for the vehicle to be able to follow the reference path. In the ideal case the inputs match the actual states. However, when using sensors the data can contain noise components which can lead to problems with the controller. Figure 55 till Figure 58 contain data plots of several simulations with noise on individual inputs of the controller. The noise is generated by a white noise signal with a bandwidth equal to the inversed sampling time of the model, which is added to the outcome of the dynamic signals for each input of the controller respectively. The noise is injected before it is used as an input for the controller. For each input the maximum noise for which the controller is able to keep the vehicle following the reference path is shown. The figures for of the noise are seen in Appendix D.

Starting with the articulation angle, the controller is able to control the vehicle with noise on the articulation angle with an amplitude of 0.4 rad. Compared to the zero noise input the noise is up to 40% of the maximum articulation angle, which causes the vehicle to steer continuously to its limits. However, the controller is capable to follow the reference path. The velocity noise can be around 0.1 m/s till the controller is unable to function. The angular velocity noise is allowed to be below 0.4 rad/s and the position noise can be at most 1.5 m before the vehicle becomes unstable. Combining these results shows that the controller can cope with large amounts of noise before the tractor-semitrailer becomes unstable (The vehicle will not be able to follow the reference path). Note, these noises were individually tested. Disturbance on all inputs combined will require the noise to be of lower amplitude. However, in general noises of the amplitudes shown in the graphs are much larger than in practice so external disturbances should not be a problem when using the controller on a real-life vehicle.

Besides the reverse driving, forward driving has to be tested in a similar way. The following tests are done with the optimal controller gains for forwards driving, which are given by a steering sensitivity of 8.6 and a look ahead gain of 3.8. Figure 42 shows the result of the horizontal offset and Figure 43 is a plot of the radial offset. As seen the forward controller cannot stabilize the vehicle when it has a lateral offset. This is caused by the high control gain and the location of the preview point. The preview point will overshoot the reference path which pushes the vehicle in a sinusoidal movement, resulting that the vehicle is not able to move back to the reference path. The radial offset can be at most 4.5 degrees before the vehicle becomes unstable.

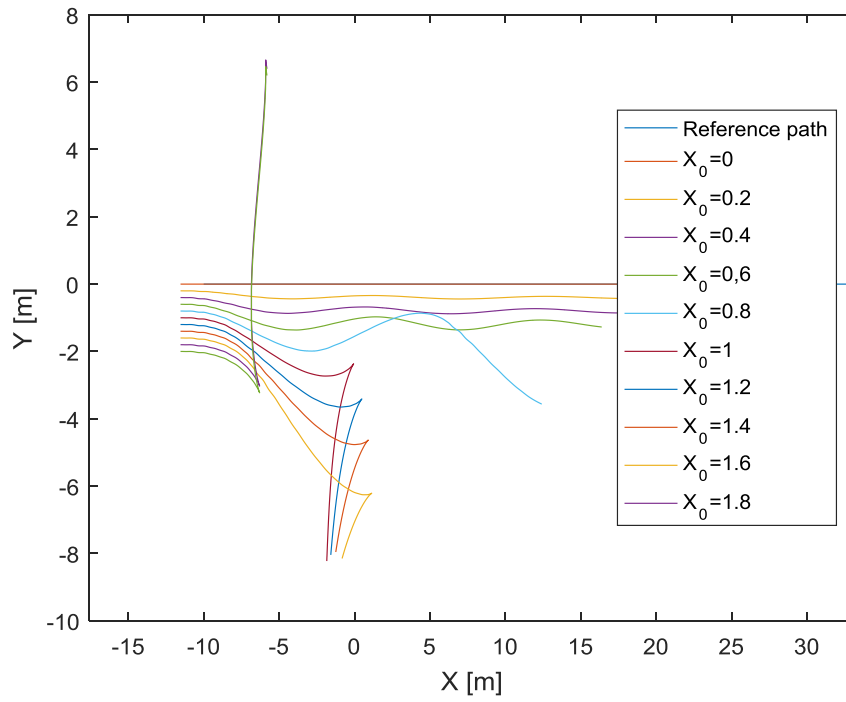


Figure 42: Y0 offset to reference path

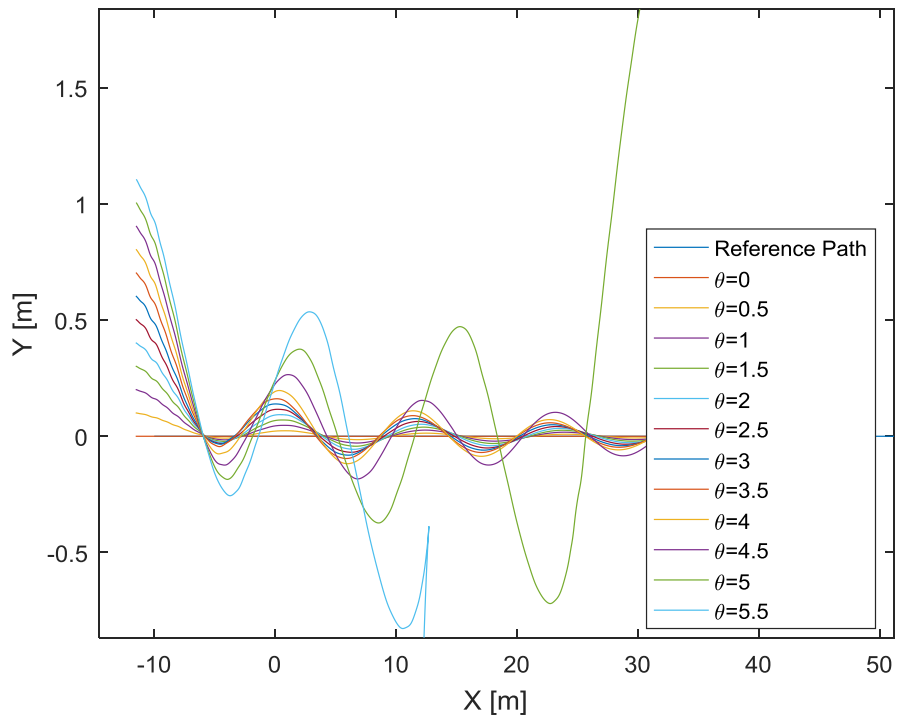


Figure 43: Angular offset to reference path

The forward driving controller has fewer inputs than the reverse situation. The velocity of the tractor and the position of the axle are the two inputs for the controller. In Appendix D simulation figures show the amplitude of noise allowed before the vehicle becomes unstable. The amplitudes of noise are similar to the reverse simulation. In this case, the noise should not be a problem when testing the forward controller on a real-life vehicle.

## 8. Double articulated vehicle combination

Shown in the previous chapters, the proposed controller can control a single articulated vehicle along a defined reference path in reverse or forward motion. However, results for different vehicle combinations are desired to show the capabilities of the path controller. In this case simulations are done for a double articulated vehicle combination. A schematic of the double semi-trailer vehicle is shown in Figure 44. It is the same as the tractor-semitrailer with an additional trailer added to the end of the vehicle

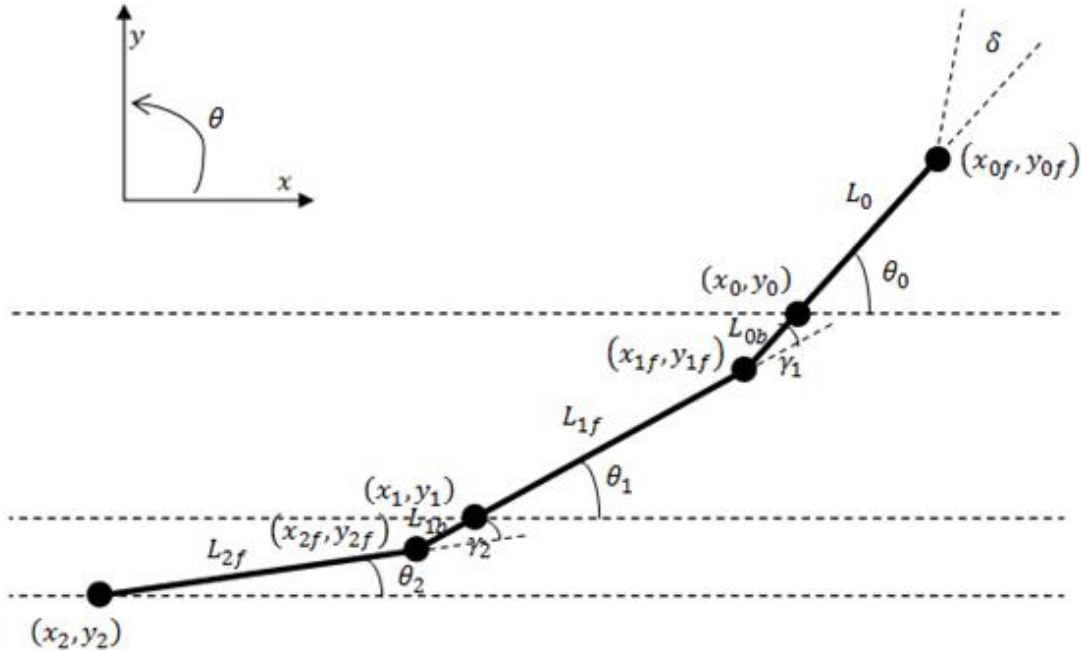


Figure 44: Kinematic model double semi-trailer vehicle

The kinematic model is a single track model, assuming a single lateral constraint on the axles of the tractor and semi-trailer. The steering angle  $\delta$  at the front of the tractor is an input to the model. The longitudinal velocity of the tractor  $v_0$  is the second input to the model, applicable for the reference point  $(x_0, y_0)$ . The heading angle of the tractor, the first trailer and the second trailer are indicated by  $\theta_0$ ,  $\theta_1$  and  $\theta_2$  respectively. The articulation angle  $\gamma_1$  is described as the difference in heading angle between tractor and the first trailer, articulation angle  $\gamma_2$  is the difference in heading angle between the first trailer and the second trailer.  $L_0$  is the wheelbase of the tractor,  $L_{0b}$  is the distance between rear of the tractor and the first kingpin  $(x_{1f}, y_{1f})$ ,  $L_{1f}$  is the distance between the first kingpin point and the axle of the first trailer  $(x_1, y_1)$ ,  $L_{1b}$  is the distance between rear of the first trailer and the second kingpin  $(x_{2f}, y_{2f})$  and  $L_{2f}$  is the distance between the second kingpin and the rear of the second trailer  $(x_2, y_2)$ .  $L_{0b}$  and  $L_{1b}$  can be either positive or negative depending on the location of the kingpin.



There are two ways of defining the extended vehicle combination. The first way is using the non-holonomic constraints as given in Chapter 2. This will result in lengthy equations which are not easily implemented in Simulink. The second way is using the model defined in Chapter 2 and extending it. The first trailer can be seen as “Tractor” and the second trailer can be seen as the first trailer. This principle is shown in Figure 45. This method allows for a simple definition of the model for the double semi-trailer combination and the kinematic translation is similarly defined as in Chapter 4.

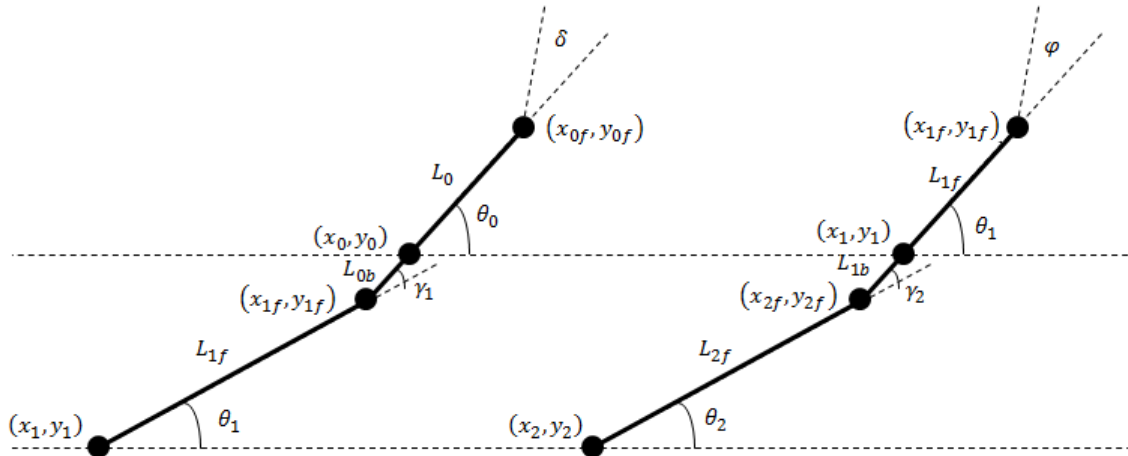


Figure 45: Separated double semi-trailer combination

The next equations that are added to the tractor-semitrailer model to get the double semi-trailer model are:

$$x_{2f} = x_1 - L_{1b} \cos(\gamma_1) \quad (8.1)$$

$$y_{2f} = y_1 - L_{1b} \sin(\gamma_1) \quad (8.2)$$

$$x_2 = x_{2f} - L_{2f} \cos(\gamma_2) \quad (8.3)$$

$$y_2 = y_{2f} - L_{2f} \sin(\gamma_2) \quad (8.4)$$

$$\gamma_2 = \theta_1 - \theta_2 \quad (8.5)$$

To get the angular velocity of the second trailer, the variables for the first trailer in Equation 2.6 can be substituted with the variables of the second trailer.

$$\dot{\theta}_2 = \frac{v_1}{L_{2f}} \left( \sin(\gamma_2) - \frac{L_{1b}}{L_1} \tan(\varphi) \cos(\gamma_2) \right) \quad (8.6)$$

To validate the model, the model is implemented in Simulink and simulated driving forwards with a certain steering angle. The following parameters are used:  $L_0 = 3.8 \text{ m}$ ,  $L_{0b} = L_{1b} = 0.74 \text{ m}$  and  $L_{1f} = L_1 = L_{2f} = 8.475 \text{ m}$ . The result is shown in Figure 46 and Figure 47, which shows that the model behaves correctly for the given inputs.

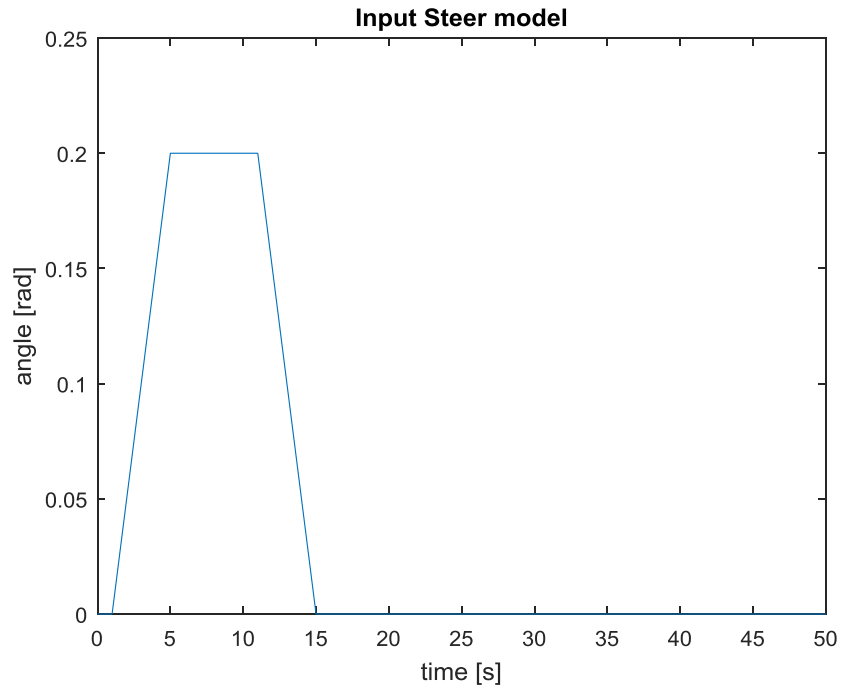


Figure 46: Steer input

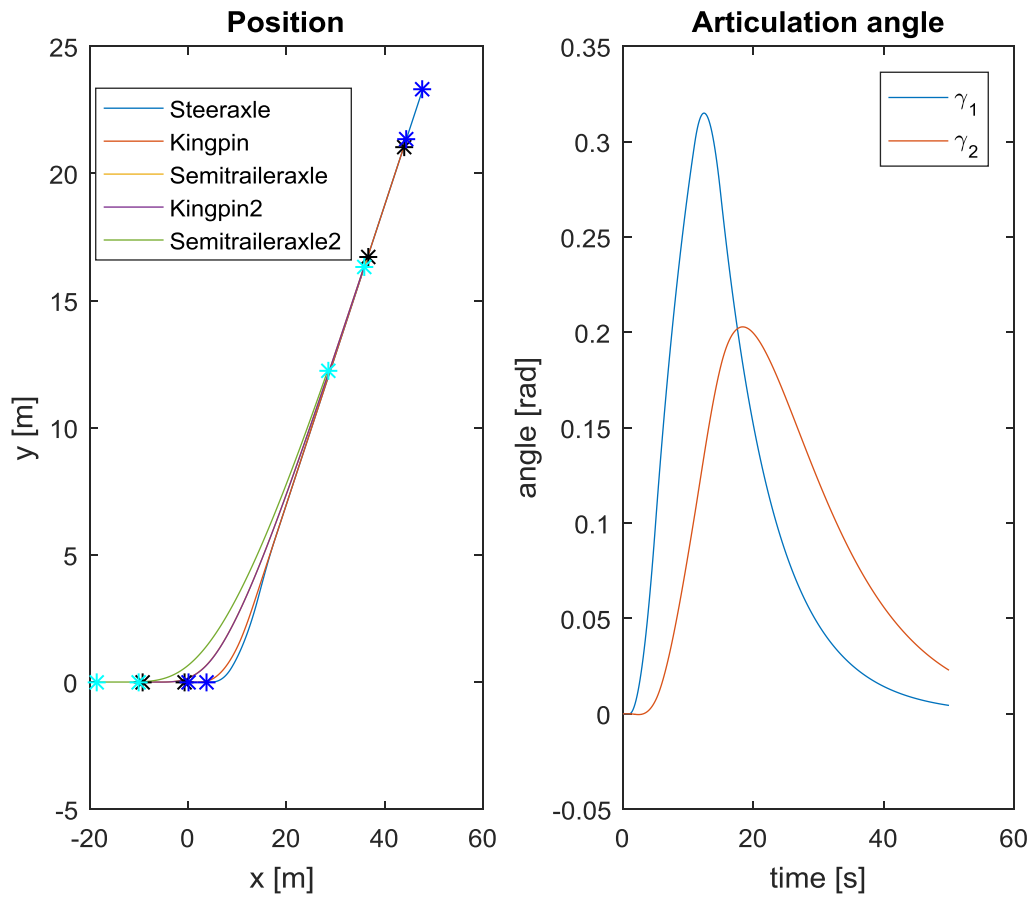


Figure 47: Result forwards simulation for double trailer model <sup>{Double articulated kinematic model}</sup>

For the controller to work, the steering translation is needed to calculate the steer input for the vehicle. Here the vehicle is separated into two parts to find the translation equations in a simple manner. The separated vehicle is shown in Figure 48.

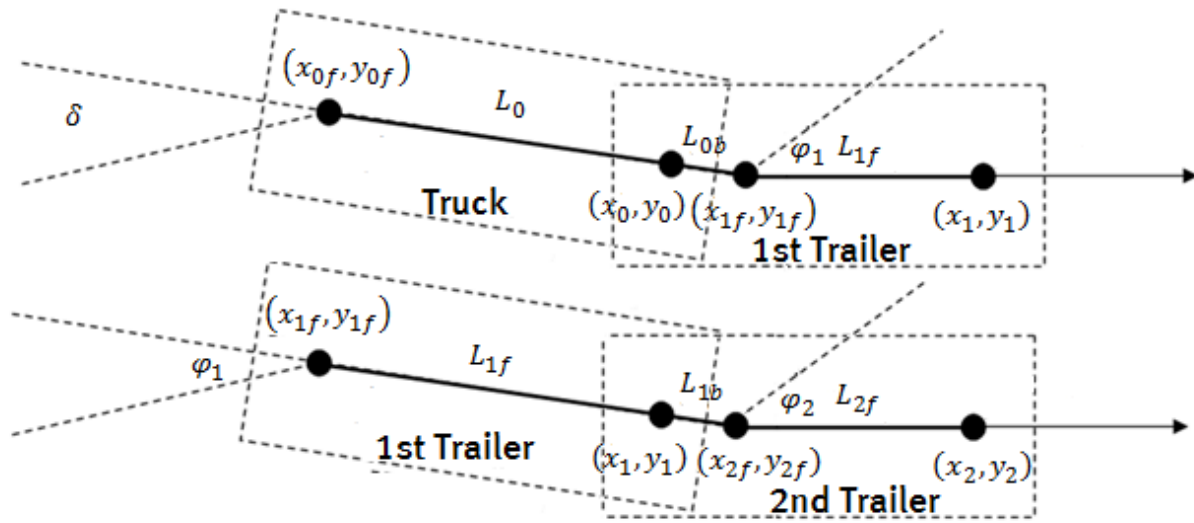


Figure 48: Steering translation for separated vehicle

Equation 8.7 shows the steering translation for the top combination of Figure 48 and is a copy of Equation 4.6. The bottom combination can be derived by substituting the variables in Equation 8.7 with the variables shown in the bottom combination. This results into:

$$\delta = \arctan \left( \left( \frac{L_0 v_1}{L_{0b} v_0} \right) (\sin(\gamma) + \tan(-\varphi_1) \cos(\gamma)) \right) \quad (8.7)$$

$$\varphi = \arctan \left( \left( \frac{L_{1f} v_2}{L_{1b} v_1} \right) \cdot (\sin(\gamma_2) + \tan(-\varphi_2) \cos(\gamma_2)) \right) \quad (8.8)$$

The total translation from  $\varphi_2$  to  $\delta$  is obtained by substituting Equation 8.7 into Equation 8.8. To verify the translation for the double semi-trailer vehicle, the double trailer combination is tested with the controller on a 90 degrees turn reference path. The values for the look ahead gain and the steering sensitivity gain are 2 and 7.5 respectively. These values were chosen because they give a decent response to the reference path. Here it is not the objective to find the optimal gains but to observe the performance of the controller with the double articulated model. As seen in Figure 49 the controller is capable to control the rear axle of the second trailer to the reference path. In this simulation  $L_{0b} = L_{1b} = 0.74$ . Note that these parameters can be either positive and negative. The controller changes by changing the sign of the outcome of the respective steering translation. This can be seen in Figure 50 and Figure 51. The controller gain were set to 2 for steering sensitivity and 7.5 for the look ahead gain. To fully test the system, the controller is also tested on the challenging reference path which was used to test the multibody model. The result is shown in Figure 52. In this simulation  $L_{0b} = L_{1b} = 0.74$ . The controller gains were tuned till the controller was able to keep the

vehicle combination on the reference path. The steering sensitivity was 2 and the look ahead gain was 7.5.

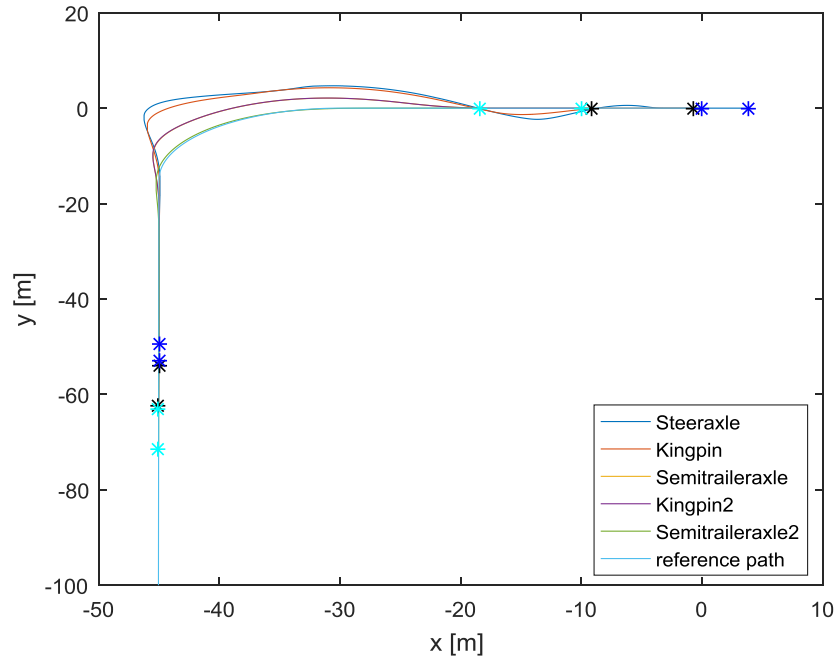


Figure 49: Double trailer simulation in reverse with a 90 degrees reference path {Double articulated kinematic model}

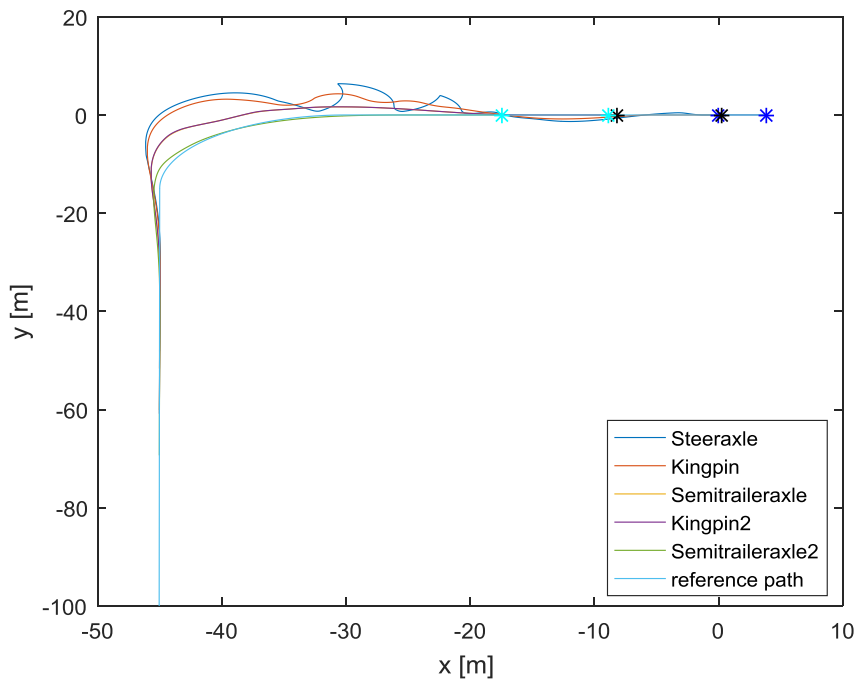


Figure 50: Double trailer simulation in reverse with  $L_{ob} = -0.3$  and  $L_{1b} = 0.74$  {Double articulated kinematic model}

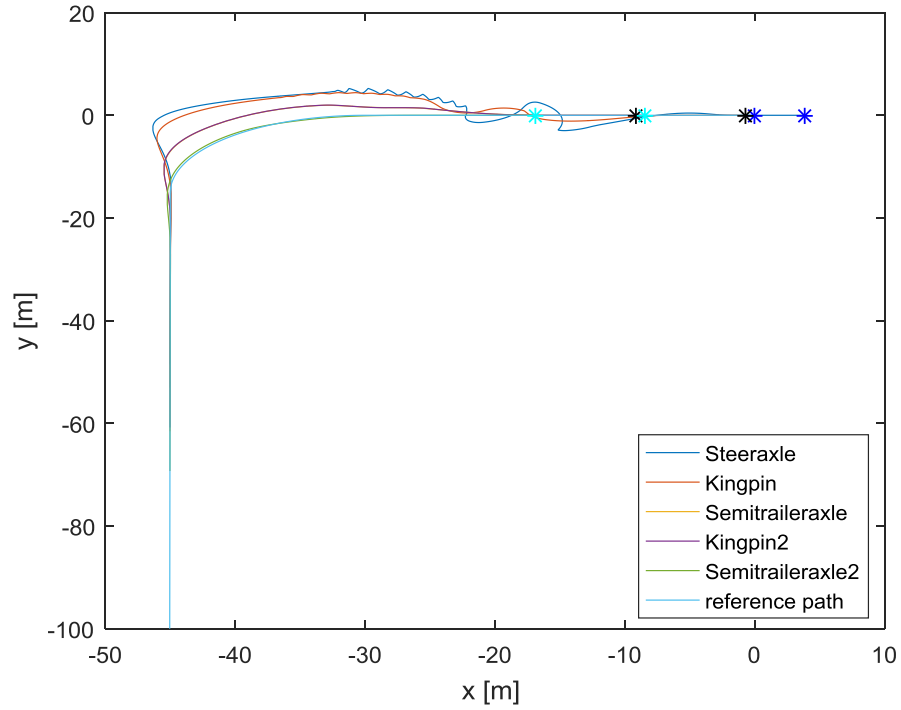


Figure 51: Double trailer simulation in reverse with  $L0b = 0.74$  and  $L1b = -0.74$  {Double articulated kinematic model}

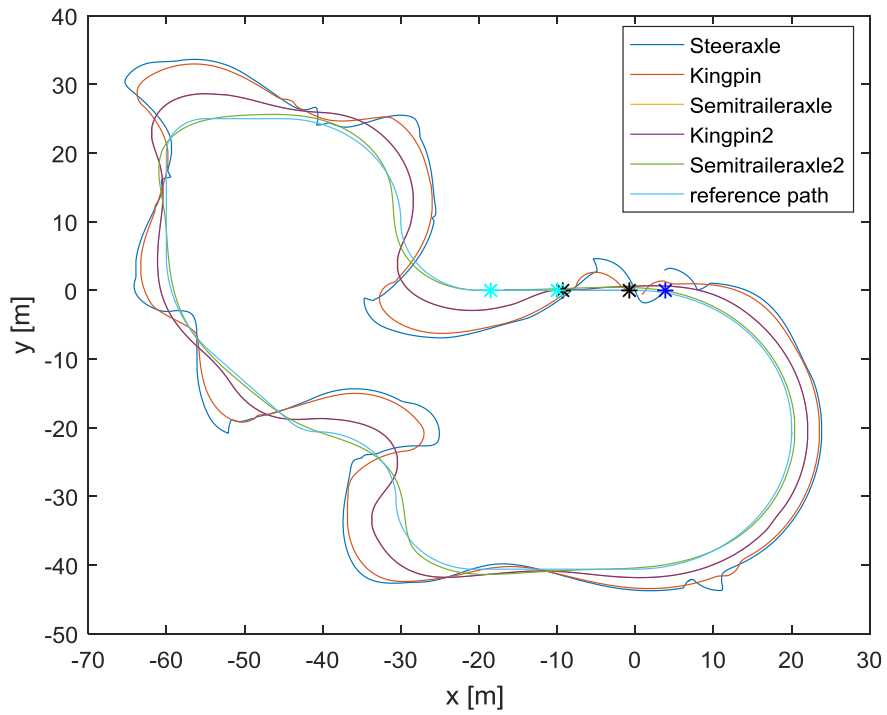


Figure 52: Two trailer model reverse on challenging reference path {Double articulated kinematic model}

## 9. Conclusions & recommendations

The single articulated kinematic model is solely based on vector calculations, while ignoring masses, inertias, friction and tire characteristics. When comparing this to the multibody model, it certainly shows a difference in response. The kinematic model reacts instantly, which allows the vehicle to be easily controlled. The multibody model needs to overcome the inertia and friction before it is able to follow the reference path, which can lead to a different.

The path controller is a very straightforward controller. In general it is a feedback controller with only proportional gains. It requires the axle positions, the radial position, the reference path and velocity of the vehicle as input and it calculates the required steering angle to follow the reference path. The controller shows very promising results for the kinematic model. The multibody model is a physical system that accurately simulates the tractor-semitrailer combination. The path following controller is able to control the multibody model to the challenging reference path. Optimal gains for this reference path were found at a steering sensitivity of 2.6 and a look ahead gain of 7.3. Note that these optimal values are specific to the reference path. When simulation the model with controller on simplified reference path, better results were found at a higher steering sensitivity up to a value of 3.5 and a lower look ahead gain of 5.5. Generally for a more difficult reference path, the look ahead gain is increased to anticipate on change in the reference path. The steering sensitivity is reduced to prevent cutting corners of the reference path. The opposite is done when the reference path; a reference path with one turn.

Noise and disturbances on the input of the controller can be of a significant value before the controller becomes unstable. For example the articulation angle can have a 30% disturbance, the positions of the tractor an error of 1 meter and the longitudinal velocity a disturbance of 10%. The initial offsets of the multibody model must be limited otherwise the controller is not able to control the vehicle to the reference path. A horizontal offset of 1.8 meter and a radial offset of 5.5 degrees are allowed.

The path controller is a very promising controller. Its concept is uncomplicated and does not require complex dynamics of the model. It requires states of the system to compute the desire input angle through kinematic relations. The disadvantage is that the controller gains have to be iteratively optimized to find desirable gains. The optimum controller gains from the challenging path (steering sensitivity is 2.6 and look ahead gain is 7.3) result into a stable vehicle for all reference paths. However, the response is not optimal for every reference path. The advantage of the controller besides its simplicity is that the semi-trailer model can be adjusted to the desired combination. For a double articulated vehicle, the controller was capable to control the vehicle to the reference path with minimal effort to extend the controller.

For future work, the path following controller can be extended with more controller gain; for example integrating components can be added to further reduce the error that the proportional

gains in the controller is not capable of. Besides the change in the controller, the vehicle configurations can be adjusted. There exist many different configurations ranging from different axle configurations to additional trailers or dollies. The controller is only tested on simulations on varies simulation models. Therefore, the controller should also be tested on tractor-semitrailer prototypes which can actually move like the simulation. Currently the controller is already tested on prototypes but much more development can be done. A certain problem can be the inputs to the controller which cannot be directly obtained on prototypes. More research has to be done on information gathering and processing of signals for these prototypes.

## 10. References

- [1] K. Patel (Oktober 2014). Driver assistance during rearward maneuvering of a Longer Heavier Vehicle, HAN University of Applied Sciences
- [2] Morales, Jesus; Mandow, Anthony; Martinez, Jorge L.; Martínez, Jorge L.; Garcia-Cerezo, Alfonso J.; , "Driver assistance system for backward maneuvers in passive multi-trailer vehicles,"2012 IEEE/RSJ International Conference on Intelligent Robots and Systems (IROS), pp.4853-4858, 7-12 Oct. 2012 doi: 10.1109/IROS.2012.6385799



## Appendix A: Single Articulated Vehicle

The positions and velocities of the tractor semi-trailer combination are given in a  $(x, y)$  coordinate system. The reference point for the vehicle is given by  $(x_0, y_0)$ , which corresponds to the rear axle of the tractor. A longitudinal velocity  $v_0$  is prescribed at the reference point as input of the system. The quantities and the units of the variables can be found in Appendix B.

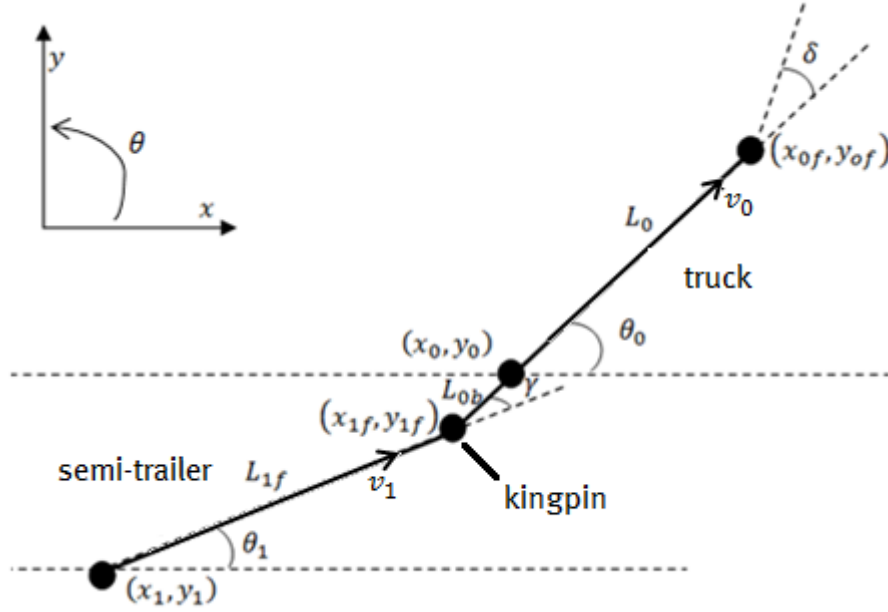


Figure 53: Single articulated vehicle model

The positions of the axels can be defined based on the reference position:

$$x_{0f} = x_0 + L_0 \cos(\theta_0) \quad (\text{A.1})$$

$$y_{0f} = y_0 + L_0 \sin(\theta_0) \quad (\text{A.2})$$

$$x_{1f} = x_0 - L_{0b} \cos(\theta_0) \quad (\text{A.3})$$

$$y_{1f} = y_0 - L_{0b} \sin(\theta_0) \quad (\text{A.4})$$

$$x_1 = x_{1f} - L_{1f} \cos(\theta_1) = x_0 - L_{0b} \cos(\theta_0) - L_{1f} \cos(\theta_1) \quad (\text{A.5})$$

$$y_1 = y_{1f} - L_{1f} \sin(\theta_1) = y_0 - L_{0b} \sin(\theta_0) - L_{1f} \sin(\theta_1) \quad (\text{A.6})$$

Differentiating the reference point and Equation (A.1-A.6) results into:

$$\dot{x}_0 = v_0 \cos(\theta_0) \quad (\text{A.7})$$

$$\dot{y}_0 = v_0 \sin(\theta_0) \quad (\text{A.8})$$

$$\dot{x}_{0f} = \dot{x}_0 - L_0 \sin(\theta_0) \dot{\theta}_0 \quad (\text{A.9})$$

$$\dot{y}_{0f} = \dot{y}_0 + L_0 \cos(\theta_0) \dot{\theta}_0 \quad (\text{A.10})$$

$$\dot{x}_{1f} = \dot{x}_0 + L_{0b} \sin(\theta_0) \dot{\theta}_0 \quad (\text{A.11})$$

$$\dot{y}_{1f} = \dot{y}_0 - L_{0b} \cos(\theta_0) \dot{\theta}_0 \quad (\text{A.12})$$

$$\dot{x}_1 = \dot{x}_0 + L_{0b} \sin(\theta_0) \dot{\theta}_0 + L_{1f} \sin(\theta_1) \dot{\theta}_1 \quad (\text{A.13})$$

$$\dot{y}_1 = \dot{y}_0 - L_{0b} \cos(\theta_0) \dot{\theta}_0 - L_{1f} \cos(\theta_1) \dot{\theta}_1 \quad (\text{A.14})$$

The articulation angle and articulation angle rate is given by:

$$\gamma = \theta_0 - \theta_1 \quad (\text{A.15})$$

$$\dot{\gamma} = \dot{\theta}_0 - \dot{\theta}_1 \quad (\text{A.16})$$

The general form of the non-holonomic constraint for a point with heading angle  $\theta$  is given by Equation A.17.

$$\dot{x} \sin(\theta) - \dot{y} \cos(\theta) = 0 \quad (\text{A.17})$$

$\dot{x}$  and  $\dot{y}$  are the velocities of the axels in the given coordinate system and  $\theta$  is the angle with respect to the x-axis. Based on Equation A.17, the non-holonomic constraints for model in Figure 53 are given by:

$$\dot{x}_{0f} \sin(\theta_0 + \delta) - \dot{y}_{0f} \cos(\theta_0 + \delta) = 0 \quad (\text{A.18})$$

$$\dot{x}_0 \sin(\theta_0) - \dot{y}_0 \cos(\theta_0) = 0 \quad (\text{A.19})$$

$$\dot{x}_1 \sin(\theta_1) - \dot{y}_1 \cos(\theta_1) = 0 \quad (\text{A.20})$$

The yaw rate of the tractor can be derived by substituting Equation A.9 and A.10 into Equation A.18.

$$(\dot{x}_0 - L_0 \sin(\theta_0) \dot{\theta}_0) \sin(\theta_0 + \delta) - (\dot{y}_0 + L_0 \cos(\theta_0) \dot{\theta}_0) \cos(\theta_0 + \delta) = 0 \quad (\text{A.21})$$

Substituting Equations A.7 and A.8 into Equation A.21 results into Equation A.22.

$$\begin{aligned} & (v_0 \cos(\theta_0) - L_0 \sin(\theta_0) \dot{\theta}_0) \sin(\theta_0 + \delta) \dots \\ & - (v_0 \sin(\theta_0) + L_0 \cos(\theta_0) \dot{\theta}_0) \cos(\theta_0 + \delta) = 0 \end{aligned} \quad (\text{A.22})$$

Equation A.22 can be simplified to:

$$\begin{aligned} & v_0 (\cos(\theta_0) \sin(\theta_0 + \delta) - \sin(\theta_0) \cos(\theta_0 + \delta)) \dots \\ & - L_0 \dot{\theta}_0 (\sin(\theta_0) \sin(\theta_0 + \delta) + \cos(\theta_0) \cos(\theta_0 + \delta)) = 0 \end{aligned} \quad (\text{A.23})$$

Known are the trigonometric identities:

$$2 \cos(a) \cos(b) = \cos(a - b) + \cos(a + b) \quad (\text{A.24})$$

$$2 \sin(a) \sin(b) = \cos(a - b) - \cos(a + b) \quad (\text{A.25})$$

$$2 \sin(a) \cos(b) = \sin(a + b) + \sin(a - b) \quad (\text{A.26})$$

$$2 \cos(a) \sin(b) = \sin(a + b) - \sin(a - b) \quad (\text{A.27})$$

With Equation (A.24-A.27), Equation A.23 can be simplified to:

$$v_0 \sin(\delta) - L_0 \dot{\theta}_0 \cos(\delta) = 0 \quad (\text{A.28})$$

By rewriting Equation A.28,  $\dot{\theta}_0$  can be expressed as:

$$\dot{\theta}_0 = \frac{v_0}{L_0} \tan(\delta) \quad (\text{A.29})$$

Using the constraint in Equation A.20, the yaw rate of the semi-trailer can be defined. Substituting Equation A.7, A.8, A.13 and A.14 into Equation A.20:

$$\begin{aligned} & (v_0 \cos(\theta_0) + L_{0b} \sin(\theta_0) \dot{\theta}_0 + L_{1f} \sin(\theta_1) \dot{\theta}_1) \sin(\theta_1) \dots \\ & - (v_0 \sin(\theta_0) - L_{0b} \cos(\theta_0) \dot{\theta}_0 - L_{1f} \cos(\theta_1) \dot{\theta}_1) \cos(\theta_1) = 0 \end{aligned} \quad (\text{A.30})$$

Equation A.30 can be simplified to:

$$\begin{aligned} & v_0 (\cos(\theta_0) \sin(\theta_1) - \sin(\theta_0) \cos(\theta_1)) + L_{0b} \dot{\theta}_0 (\sin(\theta_0) \sin(\theta_1) + \cos(\theta_0) \cos(\theta_1)) \dots \\ & + L_{1f} \dot{\theta}_1 (\sin(\theta_1) \sin(\theta_1) + \cos(\theta_1) \cos(\theta_1)) = 0 \end{aligned} \quad (\text{A.31})$$

Using the trigonometric identities given in Equation (A.24-A.27), Equation A.31 can be simplified:

$$-v_0 \sin(\theta_0 - \theta_1) + L_{0b} \dot{\theta}_0 \cos(\theta_0 - \theta_1) + L_{1f} \dot{\theta}_1 \quad (\text{A.32})$$

By rewriting Equation A.28,  $\dot{\theta}_1$  can be expressed as:

$$\dot{\theta}_1 = \frac{v_0 \sin(\theta_0 - \theta_1) - L_{0b} \dot{\theta}_0 \cos(\theta_0 - \theta_1)}{L_{1f}} \quad (\text{A.33})$$

Substituting Equations A.15 and A.29 into A.33, results into:

$$\dot{\theta}_1 = \frac{v_0}{L_{1f}} \left( \sin(\gamma) - \frac{L_{0b}}{L_0} \tan(\delta) \cos(\gamma) \right) \quad (\text{A.34})$$

## Appendix B: Articulated model variables

The table below consists of the variables used in the single articulated vehicle and the double articulated vehicle.

Variable	Quantity	Value
$v_0$	Longitudinal speed of the tractor	m/s
$v_1$	Longitudinal speed of the first trailer	m/s
$v_2$	Longitudinal speed of the second trailer	m/s
$\theta_0$	Heading angle of the tractor	rad
$\dot{\theta}_0$	Angular velocity of the tractor	rad/s
$\theta_1$	Heading angle of the first trailer	rad
$\dot{\theta}_1$	Angular velocity of the first trailer	rad/s
$\theta_2$	Heading angle of the second trailer	rad
$\dot{\theta}_2$	Angular velocity of the second trailer	rad/s
$x_0$	X-position of the rear axle of the tractor	m
$y_0$	Y-position of the rear axle of the tractor	m
$x_{0f}$	X-position of the steering axle of the tractor	m
$y_{0f}$	Y-position of the steering axle of the tractor	m
$x_1$	X-position of the rear axle of the first trailer	m
$y_1$	Y-position of the rear axle of the first trailer	m
$x_{1f}$	X-position of the first kingpin	m
$y_{1f}$	Y-position of the first kingpin	m
$x_2$	X-position of the rear axle of the second trailer	m
$y_2$	Y-position of the rear axle of the second trailer	m
$x_{2f}$	X-position of the second kingpin	m
$y_{2f}$	Y-position of the second kingpin	m
$\gamma$	Articulation angle between tractor and first trailer	rad
$\dot{\gamma}$	Articulation rate between tractor and first trailer	rad/s
$\gamma_2$	Articulation angle between tractor and second trailer	rad
$\dot{\gamma}_2$	Articulation rate between tractor and second trailer	rad/s
$\delta$	Steering angle of the tractor	rad
$\varphi/\varphi_1$	Output path following controller for single articulated vehicle	rad
$\varphi_2$	Output path following controller for double articulated vehicle	rad
$L_0$	Wheel base of the tractor	m
$L_{0b}$	Distance between rear axle of the tractor and the first kingpin	m
$L_{1f}$	Wheel base of the first trailer	m
$L_{1b}$	Distance between rear axle of the first trailer and the second kingpin	m
$L_{1f}$	Wheel base of the second trailer	m

Table B. 1: Time dependent variables for the kinematic model

## Appendix C: Single articulated vehicle for reversing

The kinematic model for reversing is similar to the single articulated vehicle discussed in Appendix A, the difference lies in the reference point. The reference point for the vehicle is given by  $(x_1, y_1)$ . A longitudinal velocity  $v_1$  acts on the reference point as input of the system. The quantities and the units of the variables can be found in Appendix B and are identical to the single articulated vehicle.

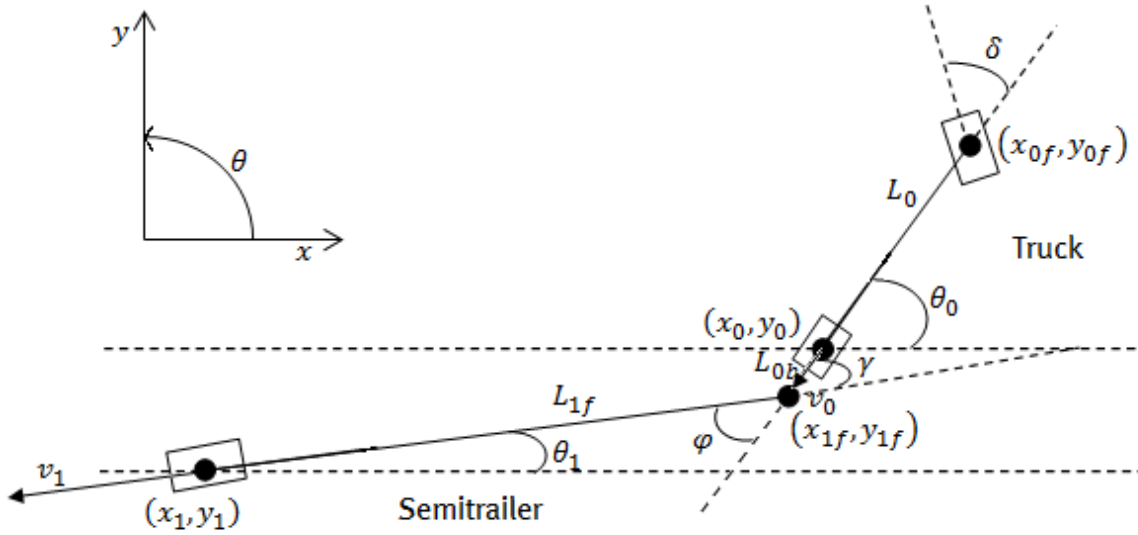


Figure 54: Single articulated vehicle model for reversing

The positions of the axels can be defined based on the reference position:

$$x_{1f} = x_1 + L_{1f} \cos(\theta_1) \quad (C.1)$$

$$y_{1f} = y_1 + L_{1f} \sin(\theta_1) \quad (C.2)$$

$$x_0 = x_1 + L_{1f} \cos(\theta_1) + L_{0b} \cos(\theta_0) \quad (C.3)$$

$$y_0 = y_1 + L_{1f} \sin(\theta_1) + L_{0b} \sin(\theta_0) \quad (C.4)$$

$$x_{0f} = x_1 + L_{1f} \cos(\theta_1) + (L_{0b} + L_0) \cos(\theta_0) \quad (C.5)$$

$$y_{0f} = y_1 + L_{1f} \sin(\theta_1) + (L_{0b} + L_0) \sin(\theta_0) \quad (C.6)$$

Differentiating the reference point and Equation (C.1-C.6) results into:

$$\dot{x}_1 = -v_1 \cos(\theta_1) \quad (C.7)$$

$$\dot{y}_1 = -v_1 \sin(\theta_1) \quad (C.8)$$

$$\dot{x}_{1f} = \dot{x}_1 - L_{1f} \sin(\theta_1) \dot{\theta}_1 \quad (C.9)$$

$$\dot{y}_{1f} = \dot{y}_1 + L_{1f} \cos(\theta_1) \dot{\theta}_1 \quad (C.10)$$

$$\dot{x}_0 = \dot{x}_1 - L_{1f} \sin(\theta_1) \dot{\theta}_1 - L_{0b} \sin(\theta_0) \dot{\theta}_0 \quad (C.11)$$

$$\dot{y}_0 = \dot{y}_1 + L_{1f} \cos(\theta_1) \dot{\theta}_1 + L_{0b} \cos(\theta_0) \dot{\theta}_0 \quad (C.12)$$

$$\dot{x}_{0f} = \dot{x}_1 - L_{1f} \sin(\theta_1) \dot{\theta}_1 - (L_{0b} + L_0) \sin(\theta_0) \dot{\theta}_0 \quad (C.13)$$

$$\dot{y}_{0f} = \dot{y}_1 + L_{1f} \cos(\theta_1) \dot{\theta}_1 + (L_{0b} + L_0) \cos(\theta_0) \dot{\theta}_0 \quad (C.14)$$

The articulation angle and articulation rate is given by:

$$\gamma = \theta_0 - \theta_1 \quad (C.15)$$

$$\dot{\gamma} = \dot{\theta}_0 - \dot{\theta}_1 \quad (C.16)$$

The general form of the non-holonomic constraint is given by Equation C.17.

$$\dot{x} \sin(\theta) - \dot{y} \cos(\theta) = 0 \quad (C.17)$$

$\dot{x}$  and  $\dot{y}$  are the velocities of the axels in the given coordinate system and  $\theta$  is the angle with respect to the x-axis. Based on Equation C.17, the non-holonomic constraints for model in Figure 54 are given by:

$$\dot{x}_{1f} \sin(\theta_1 - \varphi) - \dot{y}_{1f} \cos(\theta_1 - \varphi) = 0 \quad (C.18)$$

$$\dot{x}_0 \sin(\theta_0) - \dot{y}_0 \cos(\theta_0) = 0 \quad (C.19)$$

The yaw rate of the trailer can be defined by substituting Equation C.9 and C.10 into Equation C.18.

$$(\dot{x}_1 - L_{1f} \sin(\theta_1) \dot{\theta}_1) \sin(\theta_1 - \varphi) - (\dot{y}_1 + L_{1f} \cos(\theta_1) \dot{\theta}_1) \cos(\theta_1 - \varphi) = 0 \quad (C.20)$$

Substituting Equations C.7 and C.8 into Equation C.20 results into:

$$\begin{aligned} & (-v_1 \cos(\theta_1) - L_{1f} \sin(\theta_1) \dot{\theta}_1) \sin(\theta_1 - \varphi) \dots \\ & - (-v_1 \sin(\theta_1) + L_{1f} \cos(\theta_1) \dot{\theta}_1) \cos(\theta_1 - \varphi) = 0 \end{aligned} \quad (C.21)$$

Equation C.21 can be simplified to:

$$\begin{aligned} & -v_1 (\cos(\theta_1) \sin(\theta_1 - \varphi) - \sin(\theta_1) \cos(\theta_1 - \varphi)) \dots \\ & -L_{1f} \dot{\theta}_1 (\sin(\theta_1) \sin(\theta_1 - \varphi) + \cos(\theta_1) \cos(\theta_1 - \varphi)) = 0 \end{aligned} \quad (C.22)$$

Known are the trigonometric identities:

$$2 \cos(a) \cos(b) = \cos(a - b) + \cos(a + b) \quad (C.23)$$

$$2 \sin(a) \sin(b) = \cos(a - b) - \cos(a + b) \quad (C.24)$$

$$2 \sin(a) \cos(b) = \sin(a + b) + \sin(a - b) \quad (C.25)$$

$$2 \cos(a) \sin(b) = \sin(a + b) - \sin(a - b) \quad (C.26)$$

With Equation (C.23-C.26), Equation C.22 can be simplified to:

$$-v_1 \sin(-\varphi) - L_{1f} \dot{\theta}_1 \cos(-\varphi) = 0 \quad (\text{C.27})$$

By rewriting Equation C.27,  $\dot{\theta}_1$  can be expressed as:

$$\dot{\theta}_1 = \frac{-v_1}{L_{1f}} \tan(-\varphi) \quad (\text{C.28})$$

Using the constraint in Equation C.19, the yaw rate of the tractor can be defined. Substituting Equation C.7, C.8, C.11 and C.12 into Equation C.19:

$$\begin{aligned} & (-v_1 \cos(\theta_1) - L_{1f} \sin(\theta_1) \dot{\theta}_1 - L_{0b} \sin(\theta_0) \dot{\theta}_0) \sin(\theta_0) \dots \\ & -(-v_1 \sin(\theta_1) + L_{1f} \cos(\theta_1) \dot{\theta}_1 + L_{0b} \cos(\theta_0) \dot{\theta}_0) \cos(\theta_0) = 0 \end{aligned} \quad (\text{C.29})$$

Equation C.29 can be simplified to:

$$\begin{aligned} & -v_1 (\cos(\theta_1) \sin(\theta_0) - \sin(\theta_1) \cos(\theta_0)) - L_{1f} \dot{\theta}_1 (\sin(\theta_1) \sin(\theta_0) + \cos(\theta_1) \cos(\theta_0)) \dots \\ & -L_{0b} \dot{\theta}_0 (\sin(\theta_0) \sin(\theta_0) + \cos(\theta_0) \cos(\theta_0)) = 0 \end{aligned} \quad (\text{C.30})$$

Using the trigonometric identities given in Equation (C.23-C.26), Equation C.30 can be simplified:

$$v_1 \sin(\theta_0 - \theta_1) - L_{1f} \dot{\theta}_1 \cos(\theta_0 - \theta_1) - L_{0b} \dot{\theta}_0 \quad (\text{C.31})$$

By rewriting Equation C.31,  $\dot{\theta}_0$  can be expressed as:

$$\dot{\theta}_0 = \frac{v_1 \sin(\gamma) - L_{1f} \dot{\theta}_1 \cos(\gamma)}{L_{0b}} \quad (\text{C.32})$$

## Appendix D: Noise simulations on multibody model

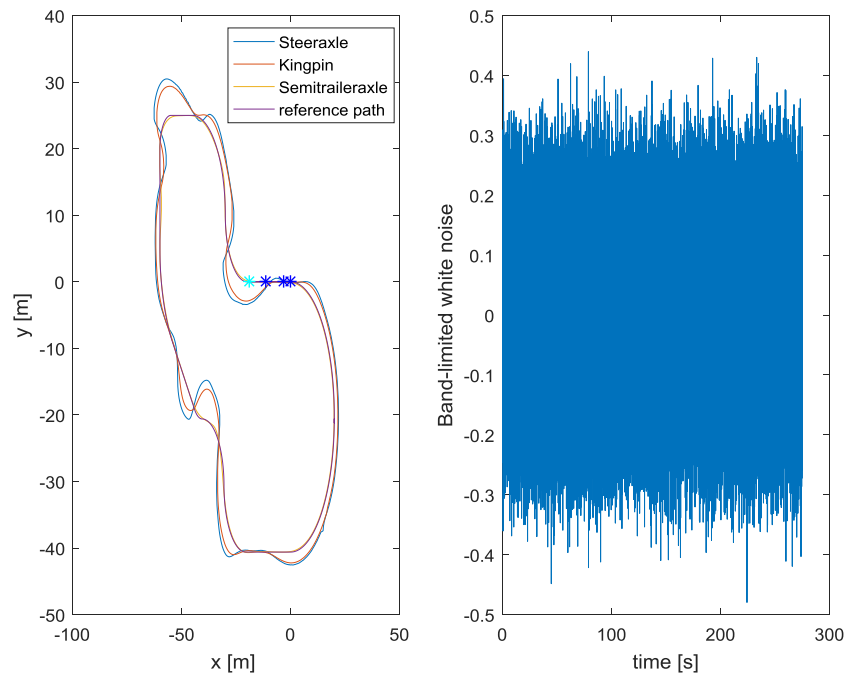


Figure 55: Reverse simulation with noise on articulation angle <sup>{Multibody model}</sup>

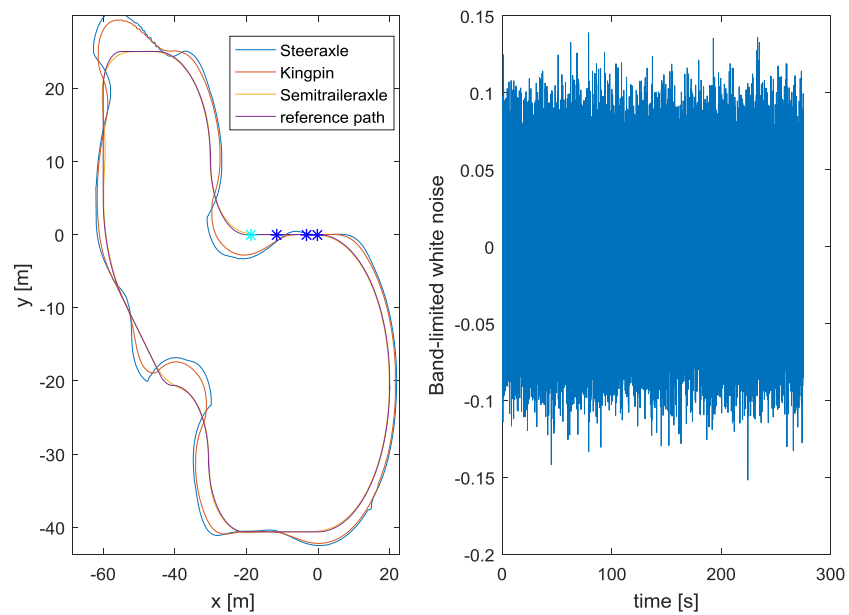


Figure 56: Reverse simulation with noise on the longitudinal velocity of the tractor <sup>{Multibody model}</sup>



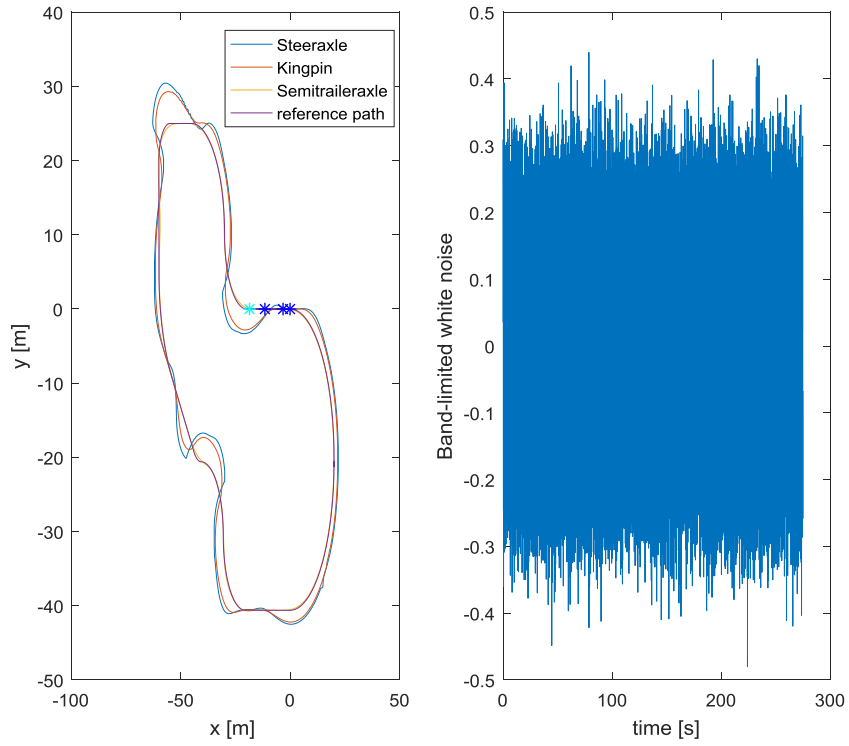


Figure 57: Reverse simulation with noise on the angular velocity of the tractor <sup>{Multibody model}</sup>

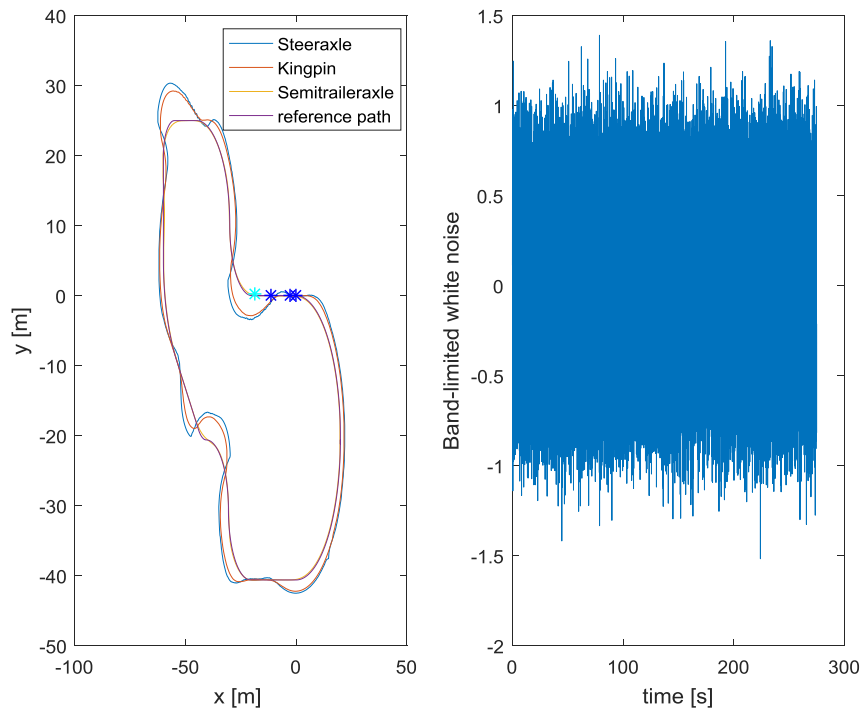


Figure 58: Reverse simulation with noise on the trailer axle <sup>{Multibody model}</sup>

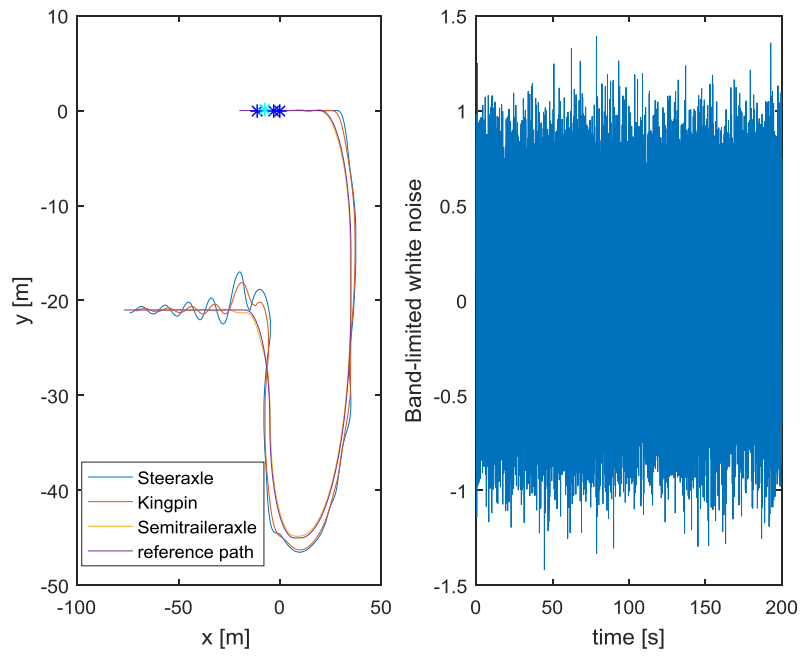


Figure 59: Forwards simulation with noise on the trailer axle <sup>{Multibody model}</sup>

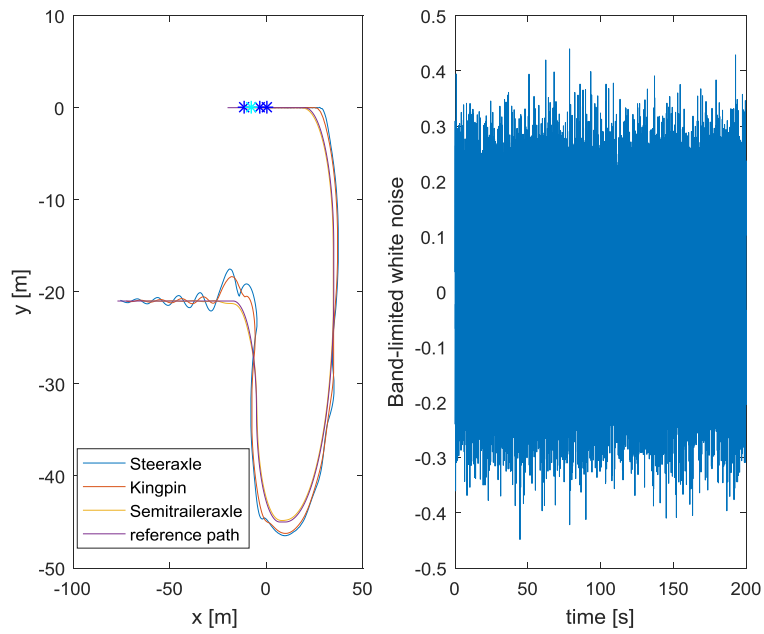


Figure 60: Reverse simulation with noise on the longitudinal velocity of the tractor <sup>{Multibody model}</sup>